NPL
National Physical Laboratory

Report

NPL REPORT
DEPC MPR 016

Review of accelerated ageing methods and lifetime prediction techniques for polymeric materials

A S Maxwell, W R Broughton, G Dean and G D Sims

NOT RESTRICTED

March 2005

dti
FUNDED BY THE DTI

National Physical Laboratory | Hampton Road | Teddington | Middlesex | United Kingdom | TW11 0LW
Switchboard 020 8977 3222 | **NPL Helpline** 020 8943 6880 | **Fax** 020 8943 6458 | **www.npl.co.uk**

dti

The DTI drives our ambition of 'prosperity for all' by working to create the best environment for business success in the UK. We help people and companies become more productive by promoting enterprise, innovation and creativity.

We champion UK business at home and abroad. We invest heavily in world-class science and technology. We protect the rights of working people and consumers. And we stand up for fair and open markets in the UK, Europe and the world.

The National Physical Laboratory is operated on behalf of the DTI by NPL Management Limited, a wholly owned subsidiary of Serco Group plc

Review of accelerated ageing methods and lifetime prediction techniques for polymeric materials

A S Maxwell, W R Broughton, G Dean and G D Sims
Engineering and Process Control Division

ABSTRACT

Manufacturers of polymer-based materials are increasingly being asked for assurance of product lifetime, particularly for components, which cannot be easily inspected or may fail catastrophically in service. Whilst the life expectancy of products in non-demanding applications have traditionally been predicted from previous in-service experience, the use of plastics in long-term or critical applications requires a far better understanding of the failure mechanisms and the use of accelerated ageing conditions to enable reliable lifetime predictions to be made. This report reviews the failure mechanisms that are commonly experienced in service and the techniques that have been developed to predict life expectancy. The report consists of: a summary of the main degradation mechanisms present in polymeric materials; a review of techniques for predicting the life expectancy of polymers; standards for life-prediction; and the results of an industrial survey examining current UK practice.

© Crown copyright 2005
Reproduced with the permission of the Controller of HMSO
and Queen's Printer for Scotland

ISSN 1744-0270

National Physical Laboratory
Hampton Road, Teddington, Middlesex, TW11 0LW

Extracts from this report may be reproduced provided the source is acknowledged and the extract is not taken out of context.

We gratefully acknowledge the financial support of the UK Department of Trade and Industry (National Measurement System Policy Unit)

Approved on behalf of the Managing Director, NPL,
by Dr M G Cain, Knowledge Leader, Materials Processing Team,
authorised by Director, Engineering and Process Control Division

CONTENTS

1 INTRODUCTION 7

2 AGEING MECHANISMS IN POLYMERS 8

2.1 THERMAL AGEING 8
2.2 WEATHERING 8
2.3 CHEMICAL DEGRADATION 9
2.4 ENVIRONMENTAL STRESS CRACKING 10
2.5 IONISING RADIATION 11
2.6 BIOLOGICAL DEGRADATION 12
2.7 CREEP 12
2.8 FATIGUE 12

3 AGEING MECHANISMS IN POLYMER COMPOSITES 12

3.1 INTRODUCTION 13
3.2 EFFECT OF MOISTURE AND WATER ON COMPOSITE PERFORMANCE 14
3.3 POLYMER MATRIX DEGRADATION 16
3.4 FIBRE DEGRADATION 17
3.4.1 Stress Corrosion of Fibres 20
3.4.2 Effects of Elevated Temperature 21
3.4.3 Effect of Other Agents 21

4 LIFE PREDICTION IN HOSTILE ENVIRONMENTS 24

4.1 THERMAL AGEING 24
4.2 TEMPERATURE-MOISTURE-STRESS SUPERPOSITION 25
4.3 WEATHERING 30
4.4 IONISING RADIATION 31

5 LIFE PREDICTION FROM CREEP BEHAVIOUR 32

5.1 INTRODUCTION 32
5.2 POLYMERS 32
5.2.1 Linear Creep 32
5.2.2 Non-Linear Creep 34
5.2.3 Time-Dependent Plasticity 36
5.2.4 Physical Ageing 37
5.3 POLYMER COMPOSITES 38

6 LIFE PREDICTION FROM FATIGUE BEHAVIOUR 41

6.1 INTRODUCTION 41
6.2 STRENGTH DEGRADATION – DETERMINISTIC APPROACH 41
6.3 STRENGTH DEGRADATION - STATISTICAL APPROACH 42
6.4 STRESS TRANSFER MODEL 44
6.5 FRACTURE MECHANICS THEORY 44
6.6 EMPIRICAL FATIGUE THEORIES 46
6.7 NORMALISED LIFE PREDICTION MODEL 47

7 STANDARD ACCELERATED AGEING TEST METHODS 51

7.1 LIQUID ABSORPTION TEST METHODS 51
7.2 THERMAL STABILITY TEST METHODS 51
7.3 ESC TEST METHODS 51

7.3.1 Introduction *51*
7.3.2 Bent Strip Tests *52*
7.3.3 Bent Strip for Flexible Materials *52*
7.3.4 Ball and Pin Impression *53*
7.3.5 Constant Tensile Deformation *53*
7.3.6 Slow Strain Rate Testing *54*
7.3.7 Constant Tensile Stress Test *55*
7.3.8 C-ring Tests *56*
7.4 WEATHERING TEST METHODS 57
7.4.1 Natural Exposure *57*
7.4.2 Artificial Exposure *57*
7.5 EVALUATION OF CHEMICAL RESISTANCE OF GRP COMPONENTS 60

8 CONCLUDING REMARKS 63

9 ACKNOWLEDGEMENTS 63

10 REFERENCES 64

APPENDIX 1 PERFORMANCE PROJECTS AND F4 CASE STUDY 68

APPENDIX 2 ISO STANDARDS 69

A2.1 PLASTICS 69
A2.2 RUBBERS 71
A2.3 COMPOSITES 72
A2.4 ADHESIVES 72

APPENDIX 3 ASTM STANDARDS 73

A3.1 PLASTICS 73
A3.2 RUBBER 74
A3.3 COMPOSITES 75
A3.4 ADHESIVES 75

APPENDIX 4 INDUSTRIAL SURVEY 77

A4.1 INDUSTRIAL SECTORS 77
A4.2 SERVICE ENVIRONMENT 78
A4.3 SHORT-TERM TESTING 81
A4.4 LONG-TERM TESTING 82
A4.5 ACCELERATED AGEING 83
A4.6 PREDICTIVE MODELLING 84

1 Introduction

Polymer and polymer composites are increasingly being used in a wide range of applications where long-term service in hostile environments is required. As a consequence, there is growing demand for manufacturers to guarantee the life expectancy of their products, particularly where inspection can be difficult or failure catastrophic. Examples of such applications include gas pipelines, chemical storage tanks, underground cabling, aerospace components, personnel safety equipment and medical implants. Stringent product guarantees are also increasingly being demanded for engineering components in products such as cars and domestic appliances, where consumers often view extended lifetime warranties as a sign of product quality. Whilst the life expectancy of products in non-demanding applications have traditionally been predicted from passed experience, the use of plastics in long-term or critical applications requires a far better understanding of the failure mechanisms to enable lifetime predictions to be made.

This Performance Programme project aims to increase confidence in the reliability of accelerated ageing techniques for polymeric materials so that costs can be reduced through optimised material selection / component design giving increased lifetimes and reduced product liability, repair and maintenance. Ultimately, the project will contribute to opening new market applications through increasing industry confidence in the use of polymeric materials in hostile environment. It is intended the final project output, a Good Practice Guide, will be a living document and will be re-issued to encompass the outputs of future programmes in order to generate a depository of accumulated experience. Later projects will be in application areas, selected on the basis of industrial demand. In the case of composites, there are few test methods or standards that predict life expectancy with confidence.

The initial stage of the project will review the existing techniques for assessing the lifetime of polymers and composites. This will include past work within DTI programmes (e.g. Performance of adhesive joints (PAJ), Composites Performance and Design (CPD), Degradation of materials in aggressive environments (DME)) and published work elsewhere. The evaluation of lifetime prediction models, protocols and standards will take advantage of research in other Performance polymer-based projects (see Appendix 1) to optimise resources and to take advantage of on-going knowledge. Included in Appendix 1 is an outline of an experimental case study forming part of this project.

This report reviews failure mechanisms commonly experienced in polymeric materials and the techniques that can be used to predict their useful service life. The review consists of the following:

- A summary of the main degradation mechanisms present in polymeric materials.
- A review of techniques for predicting the life expectancy of plastics and polymer composites.
- Standards for accelerated testing.
- An industrial survey examining current UK practice (Appendix 4).

2 Ageing Mechanisms in Polymers

2.1 Thermal Ageing

Thermal degradation refers to the chemical and physical processes in polymers that occur at elevated temperatures. Increased temperature accelerates most of the degradation processes that occur in polymers such as oxidation, chemical attack and mechanical creep. Oxidation is generally considered to be the most serious problem when using polymers at elevated temperatures[1]. The influence of temperature on the oxidation processes will depend on the chemical structure of the polymer. Thermo-oxidation is initiated by the reaction of free radicals $P^{\bullet}$ with oxygen to form peroxide radicals:

$$P^{\bullet} + O_2 \rightarrow POO^{\bullet}$$

All polymers contain these free radicals due to their polymerisation and processing history. However, the concentration of free radicals can be significantly increased by interaction with light, ionising radiation or the presence of transition metals. Once formed the peroxide radicals undergo slower propagation reactions that breakdown the polymer chains. The overall degradation process will normally involve a relatively long induction period during which little degradation is observed[1]. At the end of this period there is a rapid increase in degradation leading to a significant reduction in the mechanical properties of the polymer. This induction period is temperature sensitive and is reduced significantly at elevated temperatures. The induction period of the degradation process can normally be regarded as the serviceable lifetime of the polymer.

Other physical changes can occur in a polymer at elevated temperatures, one of the most common being thermal expansion[2]. Thermal expansion is reversible and in general does not significant affect the life expectancy of a polymer. However, in polymer composites the mismatch between the thermal expansion of the polymer matrix and the fibres may cause thermo-mechanical degradation during thermal cycling. Similar mechanisms may also occur in adhesive joints. A sudden brief exposure to high temperatures can result in a phenomenon known as thermal spiking.

2.2 Weathering

Weathering or more specifically photo-oxidation of polymers refers to the chemical and physical changes that occur when radiation is absorbed by a polymer[2-6]. Photodegradation is initiated by solar radiation, which results in the absorption of UV radiation by chromophores and in the activation of excited states in macromolecules. However, other climatic quantities such as heat, moisture and air-bourn pollution all influence the mechanisms of degradation and the subsequent results of ageing[4].

When a polymer is exposed to solar radiation the energy absorbed by the polymer results in the formation of free radicals within the polymer by the dissociation of the C-H bonds in the polymer chains.

$$PH \rightarrow P^{\bullet} + H^{\bullet}$$

The extent of this chemical reaction depends on the radiation exposure that is the quantity of ultraviolet light (<350nm) to which it is exposed. Once free radicals have been produced, reaction with oxygen generates hydroperoxides[5] (POOH).

$$P^{\bullet} + O_2 \rightarrow POO^{\bullet}$$

$$POO^{\bullet} + PH \rightarrow POOH + P^{\bullet}$$

These hydroperoxides can dissociate further to produce a series of decomposition products including aldehydes and ketones. The presence of these carbonyl groups in a degraded polymer can be used as a chemical index for degradation. Once formed these free radicals can continue to react via propagation reactions long after the initial UV exposure has ended. Termination of these free radical reactions is normally achieved through the reaction of pairs of free radicals.

$$P^{\bullet} + P^{\bullet} \rightarrow P\text{-}P$$

The formation and propagation of free radicals in itself does not serious affect the mechanical properties of the polymer, as they do not significantly alter the long-chain nature of the polymer molecules. Degradation of the mechanical properties occurs because the free radicals produced are highly unstable and readily undergo chain scission reactions. This results in the formation of two smaller polymer chains, one of which is a free radical and capable of further reactions[5].

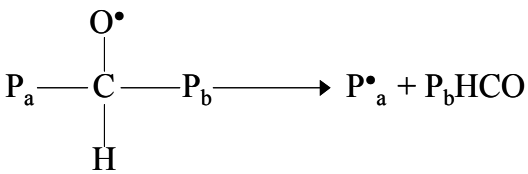

The intensity of the UV radiation decreases with increasing depth in the material, so that the reaction tends to be a near surface process. Since oxygen is involved in the reaction process, there is an important balance between UV radiation and oxygen diffusion, and of course temperature since that will also determine the kinetics of reaction and the transport of reactive species. Under natural exposure conditions there will be wetting and drying cycles and dark periods. The significance of the latter is that some recovery of the oxygen concentration in the material can occur, which otherwise is confined to the very near surface due to consumption by reaction with the polymer radicals. Since the concentration of these radicals diminishes by termination reaction during the dark period, oxygen ingress can extend to greater depth.

2.3 Chemical Degradation

Chemical attack of thermoplastics involves specific chemical reaction of the polymer with the fluid with the most common mode of failure being hydrolysis by water, acids and alkalis[2]. Esters, amides, imides, and carbonate groups are particularly susceptible. Where these groups are located in the backbone chain rather than the side chain, chain scission ensues. A general hydrolysis scheme can be summarised as follows:

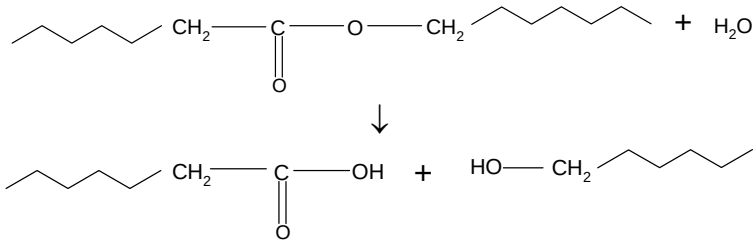

The reduction in molecular weight consequent upon chain scission can lead to a reduction of toughness and fracture strain. Stress is known to accelerate the chain scission process and also to enhance the rate of fluid uptake.

2.4 Environmental Stress Cracking

Environmental stress cracking (ESC) remains one of the most common causes of failure in polymers. The main reason for this is the complexity of the phenomenon, with aspects such as chemical compatibility, liquid diffusion, craze formation and crack development all playing their part. While crystalline and amorphous polymers are both susceptible to ESC, amorphous polymers are particularly susceptible due to their relatively open structure that leads to easy fluid penetration. Once the fluid has penetrated the polymer it becomes locally dissolved promoting cracking and crazing in the polymer. Cracking is normally preceded by the formation of crazes initiated at sites of stress concentration or at regions of local microstructural inhomogeneity. Crazes are voids that are held together by highly drawn fibrils, which bridge the void allowing the craze to transmit stress and prevent the craze from propagating. The mechanism of crazing in chemical environments is generally considered to be identical to that in air[6-8]. In general terms[9] craze initiation is considered to evolve from microdeformation processes in localised regions about 30 nm in diameter (Figure 2.1). As the deformation region develops, further localised deformation is induced. The growth and coalescence of such deformed nuclei create a narrow plastic zone. In the presence of dilatational stress, voids develop. This voided structure is considered the precursor of the fibrillated craze structure that ultimately leads to failure[10].

The environment accelerates the craze formation process by local plasticisation[7,8], i.e. enhancement of the local relative movement of molecular chains by reduced intermolecular interaction between chains. However, the particular phase of craze precursor development during which acceleration by the environment occurs, and the dependence of this on polymer type, is less clear. It has been[8] proposed that the role of the environment is to determine when the voided precursors break down to form crazes. It has been suggested also that the environment is important in void stabilisation through surface energy reduction.

Stress concentration can be important not only for the development of local deformation zones (although this is not necessarily dependent on stress concentration) but also for concentrating absorbed molecules in response to the presence of dilatational stress.

The rapid growth of the craze precursor to a visible crazes is believed to occur at a critical level of the inelastic strain which is independent of the environment and temperature[8,11,12]. This has significant implications for assessing the durability of a polymer. For example, in polymer-fluid combinations that lead to plasticisation-

induced toughening, simultaneous exposure may delay the development of crazes. However, exposure to the fluid after the sample has been stressed in air to attain the critical level of inelastic strain may lead to rapid crazing. It helps explain the very rapid development and growth of crazes in many cases when environment exposure times are relatively short but the time under stress has been long.

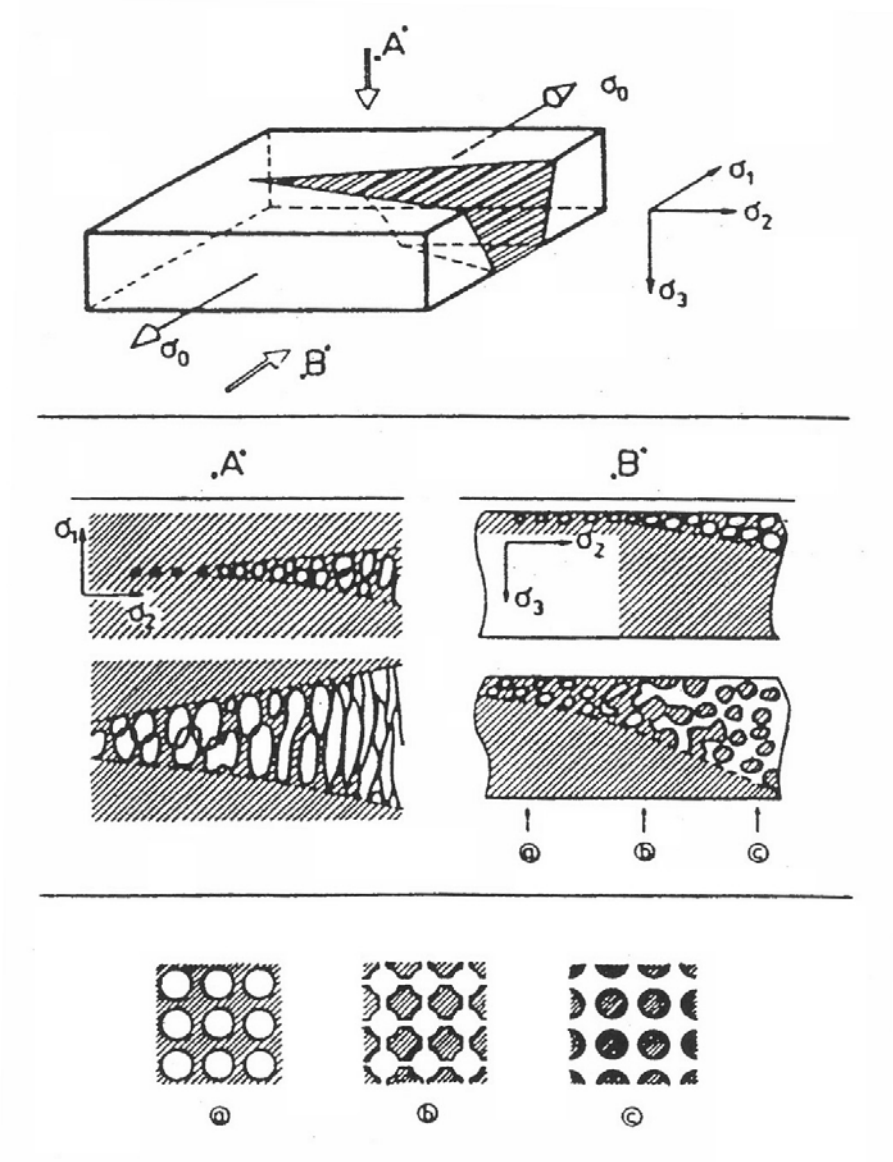

Figure 2.1 Transformation of a craze nuclei into a craze (Reference 10).

2.5 Ionising Radiation

Ionising radiation covers a wide range of different forms of radiation including x-rays, gamma rays, neutrons, alpha particles and beta particles. When a polymer is irradiated the ionising radiation induces degradation by the formation of free radicals or ions in the polymer. These reactive intermediates are capable of initiating chemical reactions which occur by free radical or ionic mechanisms and which result in scission as well as in cross-linking reactions.

Free radicals with a long lifetime, which are present in the bulk of the material after irradiation are responsible for changes in properties even a long time after exposure[13,14].

The intensity of ionising radiation on the earth's surface is not normally high enough to significantly affect most plastics, hence radiation exposure tests are only required in connection with nuclear plants and where radiation is used for applications such as medical x-rays, sterilisation or cross-linking.

2.6 Biological Degradation

Biological degradation is not a common form of degradation as most commonly used thermoplastics are resistant to microbiological attack. The only cases were biological attack has influenced life expectancy has been with certain polyurethanes and some low molecular weight additives in PVC[3]. No predictive techniques for the life expectancy of conventional polymers due to biological degradation have been developed although there are standards for testing resistance (Appendixes 2 and 3). There is, however, growing interest in the development of deliberately short-lived polymers both for medical applications and for use as disposable packaging.

2.7 Creep

Creep is the gradual increase in strain that occurs in a material when it is subjected to a constant load over an extended period of time. Viscoelastic materials, such as polymers can undergo creep at relatively low stress levels and often at temperatures below room temperature[3]. Dimensional stability under stress is essential in many applications so creep can be a significant problem. Creep will ultimately lead to rupture either by ductile or brittle failure. At low temperatures and high loads creep rupture will be brittle; at intermediate loads and temperatures failure will be ductile; and after long lifetimes slow low energy brittle failures will occur. It is these slow low energy brittle failures that are more problematic in the prediction of life expectancy.

2.8 Fatigue

Polymers will suffer failure when they are exposed to cyclic loads at stresses well below those they can sustain under static load. This phenomenon is known as fatigue and is responsible for approximately 1 in 5 of all polymer failures. The general approach to fatigue is to develop curves of applied stress (S) against the number of cycles before failure (N). These are known as S-N curves and have a characteristic sigmoidal shape, often flattening out when N is large suggesting a fatigue limit[3], although this maybe an artefact of test methodology. Unlike metals the S-N curves for plastics are extremely frequency dependent. This is due to increases in the temperature of the plastic caused by mechanical hysteresis that results in thermal softening. This means that failure under cyclic loading can be either ductile or brittle. Fatigue failures are particularly serious as there is often little visual warning that failure is imminent.

3 Ageing Mechanisms in Polymer Composites

3.1 Introduction

The extensive application of composites has seen the emergence of durability problems specific to these materials where durability relates to the long-term performance under adverse conditions, often 20 or even 50 years exposure. These problems are associated with in-service environmental conditions and handling procedures (including maintenance, repair and modifications). Durability is a serious issue from both a health and safety aspect and in terms of economic costs. The repair or replacement of a deteriorated part is both labour and capital intensive. For large structural applications, such as aircraft, bridge and offshore construction, composite parts are very expensive and due to "parts integration" are often very large. Airlines are reluctant to hold spare parts because of the cost of purchase and storage space. These problems will escalate as seating capacity of aircraft increases.

The lack of resistance of composite structures to degradation agents often becomes apparent within a short period. In some circumstances, only a few hours of exposure may lead to catastrophic failure or seriously compromise structural integrity. Irreversible property changes in polymer matrix composites PMCs can be induced by any number of degradation agents (see list below) acting alone or collectively.

- Thermal - static heat ageing, sub-zero exposure or thermal cycling
- Humidity (including hot/wet) exposures
- Complete immersion in water at ambient and elevated temperatures
- Freeze/thaw and dry/wet cyclic conditions
- Continuous or intermittent saltwater immersion or spray
- Weathering (including rain and sand erosion)
- Combined load (i.e. stress) and environmental exposures
- Chemical (including water, fuel, acids, alkalis, solvents and oxygen)
- Ultraviolet and high-energy radiation
- Electrical stress (e.g. lightning stress and galvanic reactions)
- Micro-organisms (e.g. fungi)

In many applications, composite structures will be exposed to a combination of two or more factors, often resulting in complex synergistic degradation of the material. Accelerated degradation may be caused by the combined action of two or more vectors (e.g. temperature and humidity). The relative importance of each agent will depend on the agents present and their levels. Degradation from one agent can also reduce resistance to other agents, similar to biological systems. The two predominant factors in climatic exposure are humidity and temperature. The severity of these two factors will depend on geographical location, and need to be taken into account when designing with these materials.

Failure of polymer composites, insofar as it is no longer fit for purpose, may occur because of cumulative damage to the thermoset or thermoplastic matrix, interfacial separation with the fibres, chemical attack of the fibres or a combination of two or more of these processes. The net effect is loss of stiffness and mechanical integrity. This section examines the degradation of composite materials and constituent components (i.e. fibre, matrix, fibre-matrix interface and interphase) as a result of exposure to aggressive environments.

3.2 Effect of Moisture and Water on Composite Performance

Most PMCs will absorb small, but potentially damaging amounts of moisture from the surrounding environments with the degree of degradation that occurs being linked directly with the amount of moisture absorbed. The absorbed water may adversely affect the material in a number of ways:

- Dimensional changes (swelling);
- Reduction in the glass transition temperature $\mathbf{T_g}$ of the resin; and
- Reduction in mechanical and physical properties (i.e. stiffness, strength and hardness).

In many instances, water reacts with the matrix and causes irreversible chemical changes and diminished performance. Capillary action along the fibres can account for a significant proportion of initial moisture uptake, although a chemically resistant matrix may encapsulate the fibres[15]. Shrinkage of the resin away from the fibres during curing is a contributing factor to the capillary effect. The effect of moisture is to cause hydrolytic breakdown of the fibre-matrix interface resulting in a loss in the efficiency of load transfer between the matrix and the fibre reinforcement.

The moisture absorption kinetics of polymer systems differs widely between resin systems and also changes with chemical ageing. The glass transition temperature for a typical polyester resin decreases by approximately 15-20ºC for a 2% moisture weight gain. This reduction in $\mathbf{T_g}$ is induced by plasticisation (softening) of the polymer matrix and in some cases by loss of organic additives through leaching to the surrounding media. It is advisable when using GRP products to ensure that the maximum operating temperature is at least 30-40ºC below the $\mathbf{T_g}$ of the material (taking into account moisture effects). Figure 3.1 shows the effect of moisture content on $\mathbf{T_g}$ for E-glass/F922 that has been immersed in distilled/deionised water for prolonged periods of time at three different temperatures[16].

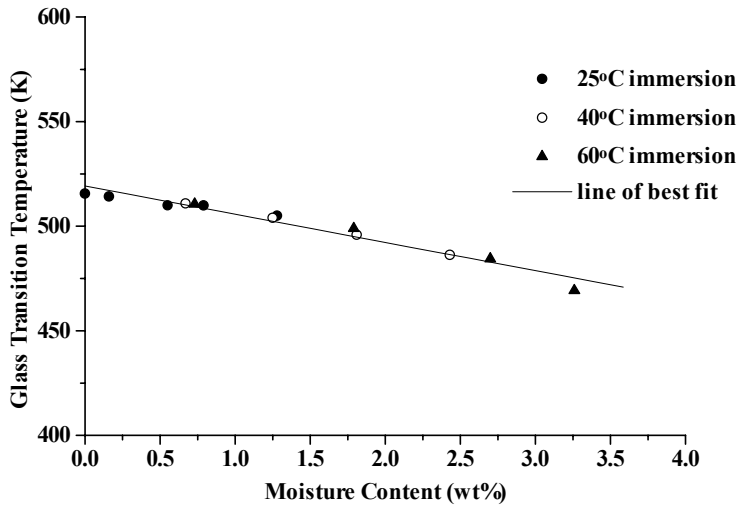

Figure 3.1: Glass transition temperature of F922 as a function of moisture content

Although the process of moisture absorption and desorption within the surface layers occurs almost immediately on contact with the environment, moisture diffusion into the bulk material is usually a slow process. It may take weeks to months before a substantial amount of moisture has been absorbed by the composite, and considerably longer periods (i.e. 1-2 years) before the material is saturated. The rate of moisture uptake by a composite laminate is dependent on the temperature, relative humidity, exposure time and mechanical load. At elevated temperatures, the rate of moisture uptake and material property degradation is accelerated.

The presence of tensile loads accelerates moisture uptake by opening existing internal cavities or voids, and by contributing to micro-crack formation. A laminate containing micro-cracks will absorb considerably more moisture than an undamaged laminate. Exposing the wet composite to sub-zero temperatures can further exacerbate this process. A commonly used test is to subject hot/wet conditioned laminates to thermal cycling in which the composite is exposed to temperatures as low as –55ºC for a given number of cycles to assess the laminates crack resistance.

All laminates when exposed to marine environments will allow water vapour to permeate the structure. As the water diffuses into the composite it reacts with any hydrolysable components (e.g. ester groups) inside the laminate to form tiny cells of concentrated solution. Under this osmotic process[17, 18] (see schematic in Figure 3.2), more water is drawn through the semi-permeable membrane of the laminate in an attempt to dilute the solution. The water can increase the fluid pressure of the cell by 50 atmospheres, which eventually distorts or bursts the laminate or gel coat and can lead to a blistering of the surface. Damage can be very extensive requiring major repair or the replacement of the structure (Figure 3.3).

Osmosis blistering is a very common problem that occurs in GRP laminated structures that have been immersed for long periods in aqueous solutions and is often observed in GRP boats, water tanks and swimming pools. A resin rich layer (e.g. gel coat) is often applied to the composite surface where the material is to be exposed for long periods to aqueous solutions. This protective layer acts as a barrier to moisture ingress, thereby protecting glass fibres from moisture degradation. Other protective measures against natural weathering include marine paint and polyurethane, which also shield the composite substrate from ultraviolet damage and weathering erosion.

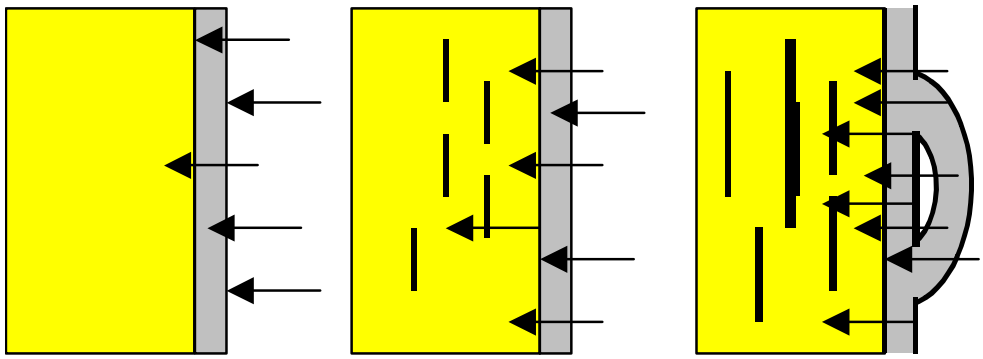

Figure 3.2: Schematic of the osmotic process – leading to delaminations/blistering

Figure 3.3: Osmotic blistering of a boat hull

Osmotic effects are amplified in the presence of hydrostatic pressure (e.g. submersibles). Entrapped air/gas/moisture vapour under pressure expands as the structure is raised from depths (as external pressure decreases), analogous to the effect of the bends experienced by divers. As a result, cracking and delaminations may occur, thus compromising structural integrity and the structures life expectancy. Porous materials can be expected to be far more prone to this effect than well-compacted materials.

The effect of moisture on aramid (e.g. Kevlar 49®) fibre-reinforced epoxy laminates is potentially greater than other composite systems. Aramid fibres tend to absorb moisture and degrade at room temperature with the rate of degradation accelerating as temperature is increased. Substantial hygrothermal strength losses have been observed with these materials, particularly under natural weathering conditions (i.e. combination of moisture and ultraviolet light).

3.3 Polymer Matrix Degradation

The polymer matrix provides a chemical barrier to the corrosive effects of moisture/water, alkalis and mineral acids, thus extending the life compared to loose fibres. Environmental stress cracking (ESC), weathering and chemical attack are the principle mechanisms for failure of the polymer matrix with the particular process being dependent on whether the matrix is a thermoplastic or thermoset and the nature of the exposure condition. ESC is an issue for thermoplastic composites and the mechanism and likelihood of attack are essentially those described for thermoplastics (section 2.4).

The majority of thermoset resins are susceptible to oxidation by numerous oxidizing agents, from exposure to elevated temperatures (i.e. thermo-oxidation), hydrogen peroxide and bleaches (e.g. hypochlorite). It is often other constituents, such as fillers, catalysts, hardeners, pigments or fire retardants, rather than the resin or fibre reinforcement that are more reactive to these chemicals. Formulators and users, although usually aware of the potential durability problems associated with these additives, often overlook minor constituents such as catalysts, hardeners, pigments and processing aids.

Most of the commonly used resin systems employed by the composite industry are far more chemical resistant to strong acids, salt solutions and oxidative agents than stainless steel or aluminium alloys. However, exposure to secondary solvents, such as paint strippers, can lead to irreversible material damage. Methylene chloride, a constituent of many paint strippers, is a known degradant of epoxy resins and other polymers.

The effect of these highly destructive processes is often evidenced by a degraded surface appearance (i.e. discolouration, loss of surface reflectivity, increased surface roughness and exposure of underlying fibres). Composites used in the automotive and aerospace industry may come in contact with aircraft fuel, gasoline, oil, hydraulic, brake and transmission fluids, lubricants, coolants and de-icing and antifreeze compounds. Many of these are known to have adverse effects on composite performance through degradation of the polymer matrix. The combination of JP-4 fuel and water is more aggressive than the two media acting alone.

3.4 Fibre Degradation

Fibre degradation is primarily an issue for glass fibres and aramid fibres, carbon fibres being stable in most environments. The tensile strength of freshly drawn E-glass fibres is typically 3.5 GPa. This strength can be fully realised, provided the fibres are carefully handled during fabrication to avoid surface damage and are stored in a dry environment. Exposure to humid air (including air-conditioned laboratories) will compromise the load bearing capacity of the fibres, resulting in a loss of strength and an increase in strength variability[19]. Carbon fibres are relatively insensitive to moisture, and hence the variability in the tensile breaking stress and strain for carbon fibre tows is noticeably less than for E-glass fibre tows.

The loss of tensile strength of E-glass fibres is dependent on exposure time, temperature and degree of humidity. On initial exposure to a humid/water environment, the rate of fibre degradation is relatively rapid, even in benign environments, such as air-conditioned laboratories. The tensile strength is reduced to 3.0 GPa after 3 weeks exposure to standard laboratory conditions (23ºC and 50% relative humidity (RH)). Immersion in water at the same temperature for the same period results in a 20% reduction (~2.5 GPa). Further strength reduction occurs with increasing exposure time. After 100 days, in air and water the strength is 2.6 GPa and 2.1 GPa, respectively[16]. Exposure to boiling water for 24 hrs results in a 75% loss of strength. As a consequence of handling and moisture, an intrinsic tensile strength of 2.0 GPa is often assumed for design purposes.

Degradation of E-glass fibres in water can be mainly attributed to leaching of alkali oxides (sodium and potassium oxide) from the fibre surface resulting in the formation of surface micro-cracks, which act as stress concentrators. The loss of strength can be expected to be permanent at all conditioning temperatures and exposure times. It is worth noting that deionised water is slightly more aggressive than either tap water or seawater.

The presence of Na^+ ions in solution slows down the exchange of alkali ions, such as $NaOH^-$, and restricts entry of Cl^- ions into the silic acid network. Chloride ions slow the degradation process, although only slightly. Under the influence of humidity or water the fibre forms a water skin in which the alkali ions (e.g. $NaOH^-$) are leached

from the fibre surface and replaced by protons (H^+). The thickness of the silic acid structure or skin increases with exposure time and is dependent on the temperature and humidity of the surrounding environment. The water surrounding the glass fibres evolves into an aggressive alkali solution as the alkali ions dissolve out of the glass, slowly decomposing the glass fibres. Increasing the alkali content of the glass tends to reduce environmental attack from water and alkali solutions.

Drying of the composite will remove most of the skin of water adjacent to the fibre, but a small permanent layer with retained water will still remain, and the mechanical properties of the fibre will be permanently degraded.

Moisture Effect on E-Glass Fibres

- **Leaching of alkali oxides (sodium and potassium oxide) from the fibre surface**

$$\text{— Si —O —R} + H_2O \rightarrow \text{— Si —O —R}^+ + OH^-$$

(R = Na, K, Ca, Mg, Al…)

- **Formation of surface micro-cracks (i.e. stress concentrators)**
- **Glass fibres slowly decompose/dissolve**
- **Permanent loss of strength (even after drying)**
- **Process accelerated with increasing <u>temperature and stress</u>**
- **Deionised water more aggressive than tap water and saltwater**

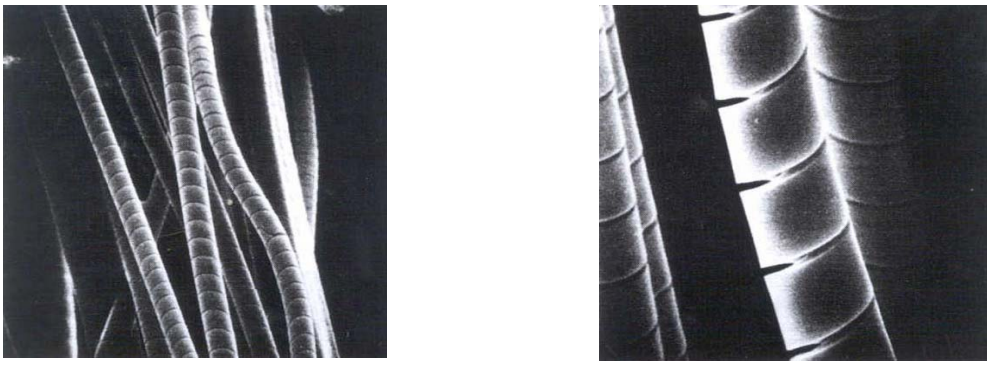

Figure 3.4: Helical cracks in E-glass fibres exposed to H_2S0_4

As with moisture effects, acid and alkali degradation processes are accelerated at elevated temperatures. Compared with other glass fibre types (e.g. R, ECR and C), E-glass is particularly vulnerable to attack from mineral acids (e.g. HCl and H_2SO_4) and alkalis (e.g. NaOH and KOH)[15]. Dilute mineral acids are not only encountered in the chemical plant industry, but are also present in industrial and household effluent and sewage. As acids come into contact with E-glass fibres, ionic exchange occurs between the metallic cations (e.g. Na^+ ions) at the glass surface and the hydrogen ions

in the acid solution, resulting in leaching of sodium, potassium, calcium, magnesium, boron and aluminium from the outer layer or sheath of the fibre.

The dissolution of the supporting network results in a slight enlargement of the fibre diameter and shortening of the fibre length as longitudinal stresses relax, which is resisted by the unaffected core. As the outer layer becomes depleted, tensile stresses imposed by the core of the fibre build up, which significantly decreases the load capability of the fibre and eventually leads to cracks (helical in shape) – see Figure 3.4. The helical nature of these cracks is due to the combination of unrestrained tangential and radial contractions. Axial cracks may also appear in the outer layer, which may spool off the fibre, like an onion peel, causing the unaffected core to be exposed. The leached outer layer is visible as a shell, which increases with time of acid exposure and eventually the glass fibres are completely leached over their entire diameter.

Mineral Acid Attack on E-Glass Fibres

- **Ionic exchange between the metallic cations (e.g. Na^+ ions) at the fibre surface and the H^+ ions in the acid solution**

$$\text{—}\ Si — O — Na + H^+ \rightarrow — Si — O — H + Na^+$$

- **Leaching of Na, K, Ca, Mg, B Al from fibre outer layer**
- **Dissolution of the silica network on fibre surface and eventually complete dissolution of fibres**
- **Slight enlargement of fibre diameter/shortening of fibre length as longitudinal stresses relax**
- **Formation of helical and axial cracks**
- **Loss of weight, strength and stiffness**

In the case of alkali attack, the chemical reaction involves a breakdown of the silica network by hydroxide (OH^-) ions and eventually dissolution of all the species in the E-glass. The glass fibres gradually lose weight and strength when they are in contact with strong alkalis. Immersion in weak caustic solutions at room temperature can result in strength reductions of 30% within 2 weeks. The rate of degradation of glass fibres to alkalis is not determined by the rate of diffusion, but by the active dissolution of the SiO_2 network. The loss of mass is proportional to time. ECR (acid corrosion resistant) glass is only slight more resistant to strong alkalis.

Alkali Attack on E-Glass Fibres

$$— Si — O — R + H_2O \rightarrow — Si — O — R^+ + OH^-$$

(R = Na, K, Ca, Mg, Al…)

$$— Si — O — Si + OH^- \rightarrow — Si —OH + — Si —O^-$$

- **Breakdown of the silica network by hydroxide (OH^-) ions**
- **Dissolution of all the species in the E-glass**

- **Fibres gradually lose weight (proportional to time) and strength**
- **Rate of degradation is not determined by the rate of diffusion, but by the active dissolution of the SiO_2 network**
- **ECR glass is only slight more resistant than E-glass to strong alkalis**

The resistance of glass fibres can be improved by modifying the chemical composition (e.g. using ECR-glass fibres for mineral acids, albeit at a high cost) or by chemical sizing (couplants, such as organosilanes) the fibre during fabrication so that there is a barrier coating, although this has limitations for some chemicals.

3.4.1 Stress Corrosion of Fibres

The process of fibre degradation is accelerated under mechanical loads with the long-term strength of GRP laminates under hostile environments being controlled by stress corrosion of the fibre-reinforcement. Static fatigue or creep rupture, which refers to time-dependent failure of the material when subjected to constant load, is used as a measure for gauging the relative resistance of the material (i.e. fibre or composite) to chemical environments. The less resistant a fibre is to a particular environment, the more rapid the drop in the rupture stress time curve. For a given applied load, the stress rupture time decreases with increasing humidity and temperature, or chemical concentration. The normalised stress rupture curves for E-glass fibres when plotted on a linear-log plot (Figure 3.5) can be approximated by the linear relationship:

$$\frac{\sigma_{APP}}{\sigma_{UTS}} = 1 - k \log t_f \qquad (3.1)$$

where σ_{APP} is the applied load (or stress), σ_{UTS} is the maximum short-term strength of the unconditioned material, k is the slope and t_f is time to failure. The constant **k** increases as the environment becomes more aggressive. Room temperature tests conducted at the National Physical Laboratory on E-glass fibre tows have shown that **k** is approximately 0.044 and 0.072 for air and deionised water, respectively.

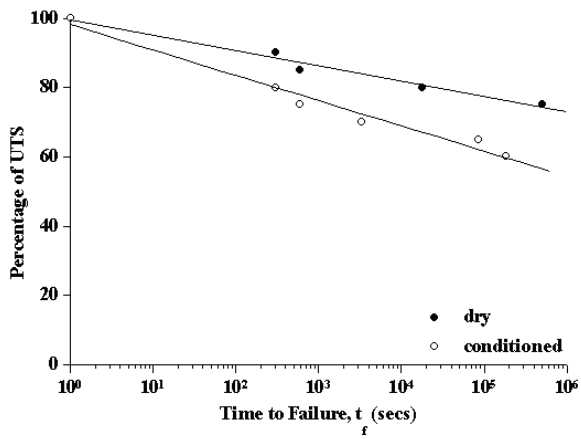

Figure 3.5: Stress rupture of E-glass fibres in air (dry) and water (conditioned)

A combination of sustained tensile load and exposure to NaOH or H_2SO_4 results in rapid failure of E-glass fibre tows. Stress rupture (failure) is almost spontaneous when fibres are subjected to 1N sulphuric acid solution at 75% of σ_{UTS} (i.e. ultimate tensile loads). In contrast, the stress rupture performance of carbon fibre-reinforced systems is far superior to that of glass fibre based systems. The creep performance under laboratory conditions is at least two orders of magnitude superior to that of glass fibre-reinforced systems. In water, the difference in stress rupture time is even greater for the same applied stress conditions.

Note: A one normal (1 N) solution contains one gram-equivalent weight of a particular substance dissolved in 1 litre of solution.

3.4.2 Effects of Elevated Temperature

Prolonged, or even short term, exposure to elevated temperatures will often produce irreversible chemical and physical changes within PMCs. As the temperature increases, the stiffness and strength decreases. All resin systems degrade at elevated temperatures. Oxidation is the primary degradation process at elevated temperatures. The rate of degradation increases with the amount of oxygen present. PMCs are permeable to atmospheric gases.

The use of anti-oxidant additives in resin systems slows the degradation process by scavenging any free radicals. Elevated temperatures also depolymerise resins and degrade the fibre-matrix interface. Differences in thermal expansivity between fibre and matrix can induce residual stresses, thereby reducing fibre-matrix bond efficiency.

3.4.3 Effect of Other Agents

A number of other degradation agents relating to in-service environmental conditions, handling and maintenance are known to have detrimental effects on the durability of composite laminates. These are discussed below.

As previously mentioned, solvents such as the paint stripper methylene chloride will soften and dissolve epoxy resins. Paint strippers combined with abrasion techniques can cause irreversible material damage. Aircraft, boats and bridges may need to be repainted repeatedly every 2-3 years during a service life, which can extend 20 to 50 years (or more). Hydraulic fluid has a similar effect to that of methylene chloride, but takes longer. Solvents such as methyl-ethyl-ketone (MEK) and acetone should not be left standing on either thermoset or thermoplastic composite surfaces.

A majority of matrix resins and carbon fibres (especially high strength fibres) are susceptible to oxidation by any one of numerous oxidising agents (e.g. hydrogen peroxide, certain bleaches such as sodium hypochlorite, nitric or sulphuric acid). Oxidation can result in loss of strength and discolouration. Atmospheric oxygen can induce degradation in matrix resins at elevated temperatures (section 3.4.2).

Intercalation is an unusual process, affecting high modulus carbon fibres, caused by chemical molecules (e.g. halogens and many inorganic salts such as ferric chloride) inserting themselves between the graphite layer planes. The result is to induce large changes in fibre dimensions.

Molecular chlorine present in aqueous solutions will cause a gradual reduction in laminate thickness (see Figure 3.6) and mechanical properties. The active form of chlorine in an aqueous solution depends on the pH of the solution, which is controlled by the following reactions:

$$\mathbf{Cl_2 + H_2O \rightarrow HClO + H^+ + Cl^-}$$
$$\mathbf{HClO \rightarrow H^+ + ClO^-}$$

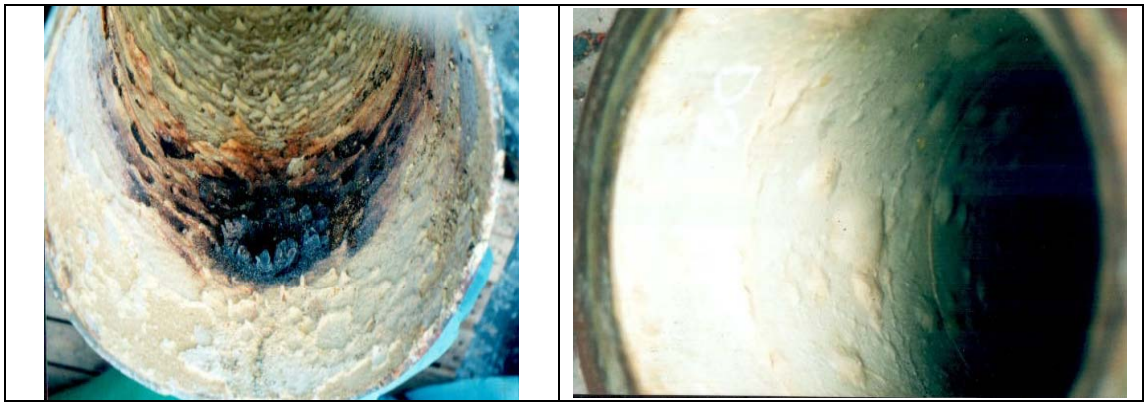

Figure 3.6: Chlorine degradation (left) and hydrogen chloride induced blistering (right) of a GRP pipe (courtesy of AEA Technology)

Ultraviolet radiation is known to degrade polymeric materials (including aramid fibres), although only the outer layer tends to be affected. Signs of photo-degradation include embrittlement (surface cracking), discolouration and loss of transparency[18]. The UV radiation spectrum comprises wavelengths of between 290 and 400 nm, which corresponds to energies of between 415 and 300 kJ/mol. These energies are in the same range as the bond energies of many organic compounds. Chemical reactions are induced when specific functional groups absorb the UV radiation. Free radicals liberated in the process will trigger further reactions. The deleterious effect will be dependent on the chemical nature of the material, environmental factors such as temperature and humidity, and exposure time. Photo-oxidative sensitivity may also increase with prolonged exposure to pollutants. Glass and carbon fibres tend to be unaffected by UV radiation. Epoxy resins are slightly sensitive to ultraviolet radiation; depending on the chemical formulation. Infrared radiation does not contribute directly to photochemical degradation, however surface heating due to the absorption of the visible infrared radiation has an indirect influence on ageing.

Galvanic corrosion occurs when two different conductive materials of different galvanic potential are in contact in the presence of water (electrolyte). The more anodic material will corrode at an accelerated rate resulting in a build up of corrosion product near the contact area. Galvanic corrosion can be a problem between carbon fibre-reinforced composite and metallic parts (aluminium alloys and steel), causing corrosion and progressive debonding in the case of honeycomb structures. The galvanic effect will be dependent on moisture content, temperature and electrical and chemical properties of the galvanic cell electrodes and electrolyte. Carbon fibre surfaces are electrochemically active supporting chemical reactions. The main reaction is cathodic reduction of dissolved oxygen to form hydroxyl ions. The reaction rate is initially controlled by the diffusion rate of the reactive components through the polymer matrix to the carbon fibre surface with the rate controlled by the type, thickness and quality of the polymer

layer and the solution chemistry. Another factor is the retained moisture in the polymer after manufacture. Once the galvanic cell is complete then the cathodic and anodic reactions initiate. The hydroxyl ions build up on the carbon fibres and react with components in the solution, such as sodium ions to balance the electrical charge. This sets up an osmotic condition as the pressure from the NaOH increases. The reaction of the composite to the osmotic pressure determines the degree of damage done to the laminate and protective polymeric layer.

4 Life Prediction in Hostile Environments

This section considers a number of non-mechanistic techniques that have been proposed to predict the residual strength and life expectancy of polymers and PMCs following exposure to combinations of heat, applied loads (static and fatigue) and moisture, or natural weathering.

4.1 Thermal Ageing

One of the most common situations that a polymer is likely to experience in service is that of prolonged exposure to elevated temperatures. The Arrhenius equation is one of the best-known models for assessing the lifetime of polymers and is commonly used to predict the combined effects of temperature and time[3]. It is particularly useful for the accelerated testing of polymers as it allows short-term tests conducted at elevated temperatures to be used to assess long-term exposures at lower temperatures.

The Arrhenius relationship is:-

$$\mathbf{K(T) = A \exp(-E/RT)} \qquad (4.1)$$

Thus:-

$$\mathbf{\ln K(T) = -E/RT + C} \qquad (4.2)$$

Where:-
K(T) is the reaction rate for the process
E is the reaction energy
R is the gas constant
T is absolute temperature
C is a constant

A plot of ln K(T) against 1/T should yield a straight line with slope E/R, which can with caution be extrapolated.

An alternative way of using the Arrhenius equation is to consider E/RT +C as a shift factor when a master curve can be built up from the material's response at different temperatures. This technique has the advantage that no particular measure of the reaction rate has to be chosen nor any form assumed for the change of parameter with time. However, considerable care has to be taken with extrapolation.

The Arrhenius relation is generally the first choice to apply to the effects of temperature but no general rule can be given for the measure of reaction rate (change of parameter with time) to be used with it. Very frequently the time taken to a given % of the initial value is chosen.

When a form of the change in parameter with time is proposed, a power law is usually tried first:-

$$\mathbf{f(X) = X^n} \qquad (4.3)$$

Combining these gives the Avrami equation:-

$$X = X_o \exp[-At^n \exp(En/RT)] \qquad (4.4)$$

Clearly other forms of reaction rate may be more appropriate.

There are occasions when the Arrhenius equation does not give a straight line and hence there is clear indication that predictions from it will not be valid. An alternative expression which has improved the line in certain cases is:-

$$\ln K = \ln K_o + B(T_o - T)/10 \qquad (4.5)$$

where: K_o is the reaction rate at a reference temperature T_o.

4.2 Temperature-Moisture-Stress Superposition

The modelling of any degradation process requires information on the change in material properties with time, and the rate of change of those properties with the level of degrading agent(s). A number of semi-empirical relationships (linear and logarithmic) for property degradation have been suggested[2,3,20,21]. These are usually of the form:

$$P(t,T) = P(\infty,T) + [\,P(0,T) - P(\infty,T)\,]\,e^{[-k(T)t^n]} \qquad (4.6)$$

where **k** is the reaction rate (or degradation rate), **P** is the material property (e.g. strength or stiffness), **T** is the ageing temperature (in K), **t** is the ageing time and **n** is an experimentally determined constant. The strength decays exponentially with time to an asymptotic value (usually zero). This approach assumes only one time-dependent process is occurring when in reality there can be several processes occurring simultaneously.

An alternative approach is to plot material property data against time for one temperature-moisture level with the data represented by one of the following empirical relations:

$$\log P(t,T) = A(T) - B(T)\,t \qquad (4.7)$$

$$P(t,T) = P(0,T)\,e^{[-k(T)t]} \Rightarrow P(\infty,T) = 0 \qquad (4.8)$$

where **B** is the degradation rate and **A** is a constant.

Similar data are generated at different temperatures. The time required for the strength to degrade to a pre-determined or limit value (usually half its original value (half-life)) at each temperature is then calculated from the fitted equations. The next step involves plotting the limit value as a function of the reciprocal of the ageing temperature (i.e. **1/T**). The half-life $t_{1/2}$ is related to the ageing temperature **T** as follows:

$$\ln t_{1/2} = C + \frac{D}{T} \qquad (4.9)$$

where **C** and **D** are material constants.

The half-life at service temperature can be estimated by extrapolation from the plot of **log $t_{1/2}$** versus **1/T** (a straight line) or by fitting the data to Equation (4.9). It is important that the test temperatures are kept moderate (< 100°C) to ensure that chemical reactions (e.g. thermal oxidation) that occur at higher temperatures are avoided, and that the dominant mode of failure is identical at all temperatures and stress levels.

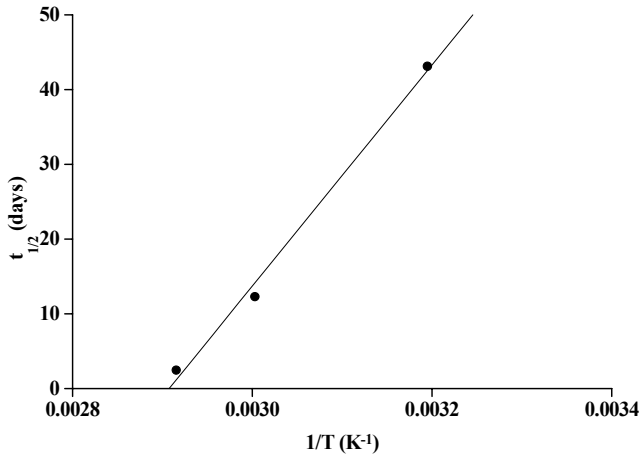

Figure 4.1: Tensile strength half-life versus temperature for E-glass/polyester

It is possible to relate the rate of strength degradation with the rate of moisture uptake (i.e. diffusivity **D**), as shown in Figure 4.1. The diffusivity **D** is a function of absolute temperature **T** and is given by the Arrhenius relation:

$$\mathbf{D = D_o \exp^{-E/RT}} \tag{4.10}$$

$\mathbf{D_o}$ is a constant, **E** is the activation energy of diffusion and **R** is the ideal gas constant.

The relationship between half life, $\mathbf{t_{1/2}}$, and diffusivity, **D**, can be approximated by the following empirical relationship (see Figure 4.2):

$$\mathbf{\ln t_{1/2} = A - BD} \tag{4.11}$$

where constants **A** and **B** are derived from line of best fit.

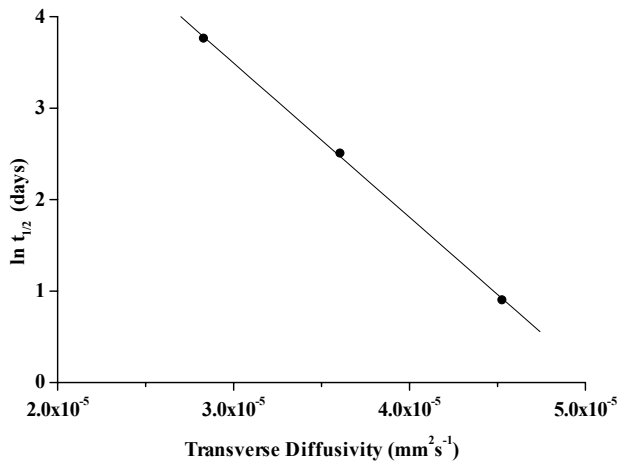

Figure 4.2: Tensile strength half-life versus diffusivity for E-glass/polyester

The above approach has been extended to determining the combined effect of temperature, moisture and stress with the failure time $\mathbf{t_f}$ given by[21]:

$$\log t_f = C - \log T + \frac{\Delta H}{2.303\,RT} - b\frac{S}{T} \qquad (4.12)$$

where **C** and **b** are constants, **T** is absolute temperature, **ΔH** is the activation energy, **R** is the universal gas constant, **T** is the absolute temperature (in K) and **S** is the uniaxial stress. At constant temperatures, the $\mathbf{\log t_f}$ versus **S/T** relation is a straight line.

Strength and stiffness property degradation due to the effects of hygrothermal ageing can be approximated using a simple algebraic relationship of the form[22]:

$$\frac{P}{P_o} = \left(\frac{T_{gw} - T}{T_{gd} - T_o}\right)^n \qquad (4.13)$$

P denotes the material property (usually strength) at the test temperature **T**, $\mathbf{P_o}$ is the initial property (un-aged) value of the dry material at room or reference temperature $\mathbf{T_o}$, and $\mathbf{T_{gd}}$ and $\mathbf{T_{gw}}$ are the glass transition temperatures of dry and conditioned (i.e. wet). The exponent **n** is a constant empirically derived from experimental data. The relationship will only provide a rational solution when $\mathbf{T_{gd} > T_o}$ and $\mathbf{T_{gw} > T}$.

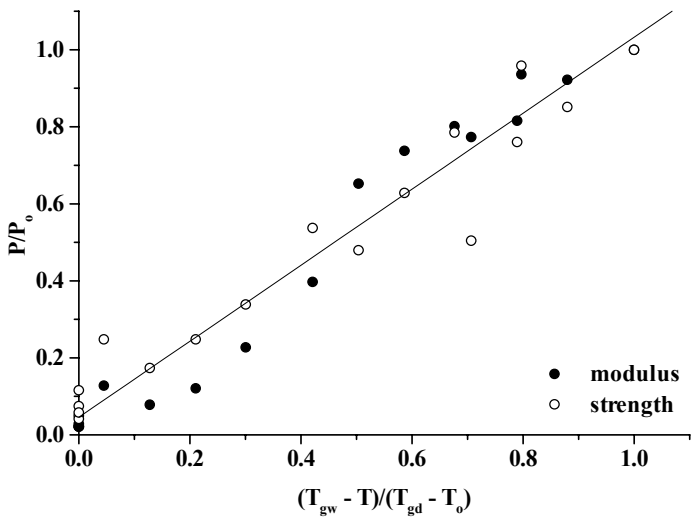

Figure 4.3: Transverse flexure properties of unidirectional E-glass/913

The good agreement between predicted and measured transverse flexure properties shown in Figure 4.3 is understandable as the power-law formula was originally intended for estimating hygrothermally-degraded properties of the resin matrix. Hence, the relationship can be expected to apply to matrix-dominated properties, such as transverse flexure and shear stiffness and strength, provided the integrity of the fibre-matrix interface is not compromised. Fibre dominated properties are less sensitive to changes in matrix properties, and hence there is poorer agreement between experimental data and estimates made using this approach and the value of the exponent **n** will differ for the stiffness and strength data.

The matrix and fibre strength and stiffness properties determined using Equation (4.13) when incorporated into micromechanics formulas (e.g. Halpin-Tsai equations) could potentially be used to derive ply stiffness and strength properties for laminate analysis. An increase in moisture content generally causes mechanical properties to decrease, although mechanical properties have been known to increase with moisture uptake. In these cases, residual stresses that have been produced in the laminate during the curing process are relieved through moisture plasticisation of the resin matrix.

Equation (4.13) can be extended to include a component for cyclic fatigue as shown below[22]:

$$\frac{\mathbf{P}}{\mathbf{P_o}} = \left(\frac{\mathbf{T_{gw}} - \mathbf{T}}{\mathbf{T_{gd}} - \mathbf{T_o}} \right)^{\mathbf{n}} - \mathbf{k} \log \mathbf{N} \qquad (4.14)$$

where **k** is obtained by curve-fitting experimental data and **N** is the number of cycles. The value of constant **A** will depend on the resin system, fibre type and orientation, and loading mode.

The wet glass transition temperature $\mathbf{T_{gw}}$ can be determined using the following quadratic relationship[22]:

$$\mathbf{T_{gw} = (AM^2 + BM + C)\ T_{gd}} \tag{4.15}$$

where **M** is the moisture content (wt %), and **A**, **B** and **C** are constants obtained by curve fitting experimental data.

For a number of materials (see Figure 4.4), $\mathbf{T_{gw}}$ and $\mathbf{T_{gd}}$ are related as follows[23]:

$$\mathbf{T_{gw} = T_{gd} - gM} \tag{4.16}$$

where **g** is temperature shift (in K) per unit moisture absorbed.

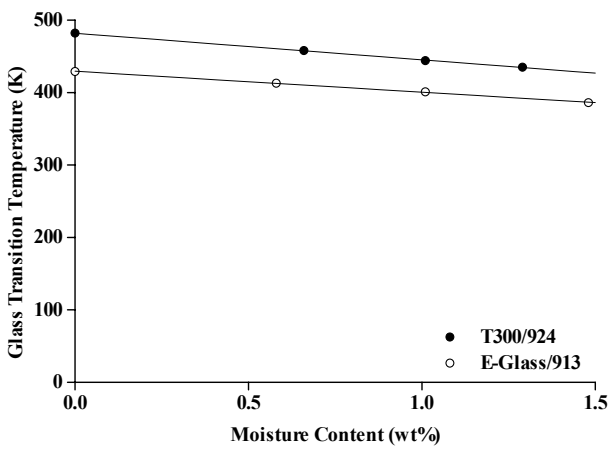

Figure 4.4: T_g versus M for hygrothermal aged unidirectional laminates

The plasticising effect (i.e. reduction of $\mathbf{T_g}$) of absorption of a diluent, such as moisture, into a composite laminate can be described by[24]:

$$\mathbf{T_g = \frac{\alpha_m T_{gm}(1 - V_f) + \alpha_f V_f T_{gf}}{\alpha_m (1 - V_f) + \alpha_f V_f}} \tag{4.17}$$

where $\mathbf{T_{gm}}$ and $\mathbf{T_{gf}}$ are the glass transition temperatures of the fibre and matrix respectively, $\boldsymbol{\alpha_m}$ and $\boldsymbol{\alpha_f}$ are thermal expansivity values and $\mathbf{V_f}$ is the fibre volume fraction.

A model developed by Bowden and co-workers[25] to predict the yield behaviour of glassy polymers has been expanded and generalised by Kittagawa[26] to provide a relationship between shear yield stress, $\boldsymbol{\tau_y}$, and shear modulus, **G**. This relationship is in the form of a power law given by[26]:

$$\mathbf{\frac{T_o \tau_y}{T \tau_{yo}} = \left(\frac{T_o G}{T G_o}\right)^n} \tag{4.18}$$

where $\mathbf{T_o}$ is the reference temperature (in K), $\boldsymbol{\tau_{yo}}$, and $\mathbf{G_o}$ are the shear yield stress and the shear modulus at reference temperature $\mathbf{T_o}$ (usually room temperature) respectively, and the exponent **n** is a constant. The values of $\mathbf{\log (T_o \tau_y / T \tau_{yo})}$ are

plotted against those of **log (T_oG/TG_o)**, such that the exponent **n** is the gradient of the linear regression fit through the log-log data. The Kittagawa power-law relationship is applicable to both shear and flexural properties of unidirectional carbon/epoxy and glass/epoxy composites[23, 27].

A number of factors may provide difficulties in interpretation of property-time measurements. These include:

- Strength may increase or decrease upon initial exposure to elevated temperatures. This may result from loss of volatiles, chemical cross-linking or relief of internal stresses.

- Long-term degradation rate may change during the ageing period. The ageing process may also change with temperature and exposure time.

- Statistical variability, which generally increases with exposure time, can introduce anomalous effects that make it difficult to differentiate the effects of key variables and to determine the ageing sequence. Rigorous statistical analysis is required to determine the precision (confidence limits) of the durability data.

- It is virtually impossible to duplicate service conditions using accelerated ageing procedures, particularly as realistic environments include large random variations in temperature and humidity.

4.3 Weathering

Weathering is of considerable complexity due to natural fluctuations in temperature, humidity, ultraviolet radiation and other environmental factors, and to the interaction of these factors, and is therefore impossible to simulate. Attempts have been made to determine the rate of degradation of a material property **P** due to the combined effect of temperature and sunlight in a similar manner to temperature-moisture superposition relations. A number of empirical relations have been proposed[2,3,4,5]:

Linear (without temperature effects)

$$\mathbf{P = P_o + bD} \tag{4.19}$$

where $\mathbf{P_o}$ is the initial property value, **D** is the ultraviolet radiation dose and **b** is a constant.

Linear with temperature effects (i.e. Arrhenius relationship)

$$\mathbf{P = P_o + De^{(-\Delta H / RT)}} \tag{4.20}$$

Power law (without temperature effects)

$$\mathbf{P = P_o + bD^n} \tag{4.21}$$

where **n** is a constant.

Exponential (without temperature effects)

$$\mathbf{P = P_o + Ae^D} \tag{4.22}$$

where **A** is a constant.

The above relations only apply to one set of conditions, and therefore extrapolating short-term data to long-term property prediction is ill advised.

A further approach is to start with a relation of the form:-

$$\mathbf{P = f(y_1 + y_2 + y_3 \ldots\ldots + y_n)}$$

Where y_1 etc. represent the various factors or agents, which may cause degradation, e.g. dosage, intensity, temperature, humidity.

Regression analysis techniques can then be used to find the significant agents and produce a model for the particular data in question. This is essentially an empirical approach. Alternatively a mathematical form for the data could be found using neural networks or curve fitting without giving consideration for the effect that individual agents have on the process. However, extrapolation of the data is then particularly dangerous.

In many weathering trials results are only available for one set of conditions and strictly no extrapolation can be made for temperature and the degradation is assumed to be independent of dosage rate.

4.4 Ionising Radiation

The effects that ionising radiation have on the properties of plastics can be predicted using a time-temperature-dose rate superposition principle[28,29,30]. This model is based on the Arrhenius expression and allows plots of degradation versus time obtained at different temperatures to be displaced along the time axis and superimposed upon one another using the following expression for the shift factor a_T:

$$a_T = \exp\left[\frac{E_a\left(T_{ref}^{-1} - T^{-1}\right)}{R}\right] \tag{4.23}$$

where T_{ref} and T are the reference and service temperatures respectively, E_a is the activation energy for the process and R is the gas constant. Burnay[30] has shown that a similar shift factor can also be used for the dose rate. Three different methods for extrapolating from high dose rates to those more typically found in service are given in IEC 61244-2[31].

5 Life Prediction from Creep Behaviour

5.1 Introduction

Creep is the increase in strain or deformation of a material with time when the material is subjected to a constant load for an extended period of time (i.e. time-dependent deformation). The change of strain at any time increases with load, temperature and relative humidity. Viscoelastic materials, such as thermoplastics and adhesives, can undergo creep deformation at relatively low stress levels (well below the ultimate strength of the material) and low temperatures (i.e. room temperature - referred to as cold flow). This can lead to considerable reduction in life expectancy of the component. Strain (or deformation) increases with load, temperature, relative humidity and time.

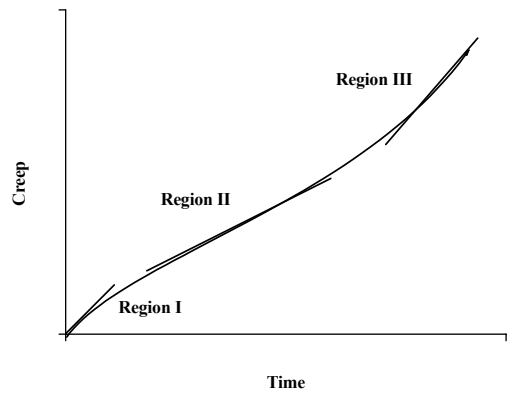

Regions

Region I – First stage, or primary creep, starts at a rapid rate and slows with time.

Region II – Second stage (secondary) creep has a relatively uniform rate (minimum gradient).

Region III – Third stage (tertiary) creep has an accelerating creep rate and terminates by failure of material at time for rupture.

It is therefore important to be able to predict the effects of long-term loading on deformation and failure behaviour. Confidence in predictions requires the use of models that accurately describe the deformation behaviour of the polymeric materials - accounting for non-linear creep under multi-axial stresses. The non-linearity arises because of a progressive reduction, with stress level, in the relaxation times of molecular relaxation processes, which account for the creep deformation. This section examines modelling of creep behaviour of polymeric materials.

5.2 Polymers

5.2.1 Linear Creep

Combinations of spring and viscous dashpot elements in series and parallel (e.g. Maxwell and Voigt models) may be used to model the time-dependent, viscoelastic behaviour of polymeric materials. The spring and dashpot configuration shown in Figure 5.1 accommodates short-term, elastic or unrelaxed response as well as a long-term, limiting deformation corresponding to a fully relaxed state[32].

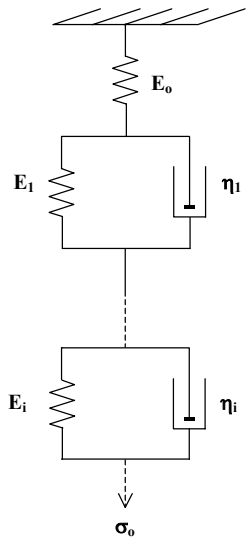

Figure 5.1: A spring and dashpot model for linear creep in polymers

For a model consisting of the 3 elements $\mathbf{E_o}$, $\mathbf{E_1}$ and $\boldsymbol{\eta_1}$, the strain response $\boldsymbol{\varepsilon(t)}$ to a constant stress $\boldsymbol{\sigma_o}$ is[32]:

$$\varepsilon(t) = \frac{\sigma_o}{E_o} + \frac{\sigma_o}{E_1}\left(1 - \exp - \left(\frac{t}{\tau_1}\right)\right) \tag{5.1}$$

where the relaxation time $\boldsymbol{\tau_1}$ is given by[32]:

$$\tau_1 = \frac{\eta_1}{E_1} \tag{5.2}$$

The single relaxation time model given above is too simplistic and is unable to describe the actual relaxation processes that occur in polymers, which have a very broad distribution of relaxation times. This model can be extended, through the incorporation of additional spring and dashpot (Voigt) elements in series to broaden the spectrum of relaxation times, and hence the time span of the relaxation process being modelled. The strain response with the inclusion of these additional elements to an applied stress is[32]:

$$\varepsilon(t) = \frac{\sigma_o}{E_o} + \sigma_o \sum_{i=1}^{n} \frac{1}{E_i}\left(1 - \exp - \left(\frac{t}{\tau_i}\right)\right) \tag{5.3}$$

where there are **n** Voigt elements in the model.

The large number of parameters that need to be determined in this model is inconvenient and is usually not necessary for modelling creep in glassy polymers at temperatures well below the glass transition temperature $\mathbf{T_g}$.

Creep strains for glassy polymers can be described by a simpler expression:

$$\varepsilon(t) = \frac{\sigma_o}{E_o} \exp\left(\frac{t}{t_o}\right)^m \tag{5.4}$$

This function will only model the short-time tail of the relaxation function given by Equation (5.3), but this is usually a valid approximation, even for extended periods under load, provided the measurement temperature is not close to $\mathbf{T_g}$. In Equation (5.4), the exponent **m** characterises a broad spectrum of relaxation times whose mean or effective value is $\mathbf{t_o}$. The equation can also be expressed as a creep compliance function **D(t)** where[33]:

$$D(t) = \frac{\varepsilon(t)}{\sigma_o} = D_o \exp\left(\frac{t}{t_o}\right)^m \tag{5.5}$$

The magnitude of the parameter $\mathbf{t_o}$ is dependent on temperature, stress level and stress state. The dependence on stress level gives rise to non-linear creep behaviour. The magnitude of $\mathbf{t_o}$ also depends on the state of physical ageing of the adhesive at the time of the creep loading.

For semi-crystalline polymers, such as polypropylene and polyethylene, where the temperature is close to $\mathbf{T_g}$, an alternative approach is to employ the Williams-Watts equation[34]:

$$D(t) = D_o + \Delta D\left(1 - \exp\left[-\left(\frac{t}{t_o}\right)\right]^m\right) \tag{5.6}$$

It should also be noted that the Williams-Watt function might not fit experimental data for all semi-crystalline polymers.

5.2.2 Non-Linear Creep

At short creep times, the compliance curves exhibit slight non-linearity. This non-linear behaviour increases significantly with time under load. At higher stresses, the creep curves are observed to shift to shorter times. Figure 5.2 shows creep compliance curves for DP460 epoxy adhesive at different stress levels. The shift to shorter times is attributed to an increase in molecular mobility brought about by the application of elevated stresses that results in a reduction in the mean relaxation time $\mathbf{t_o}$. It is the enhanced mobility that gives rise to non-linear creep behaviour.

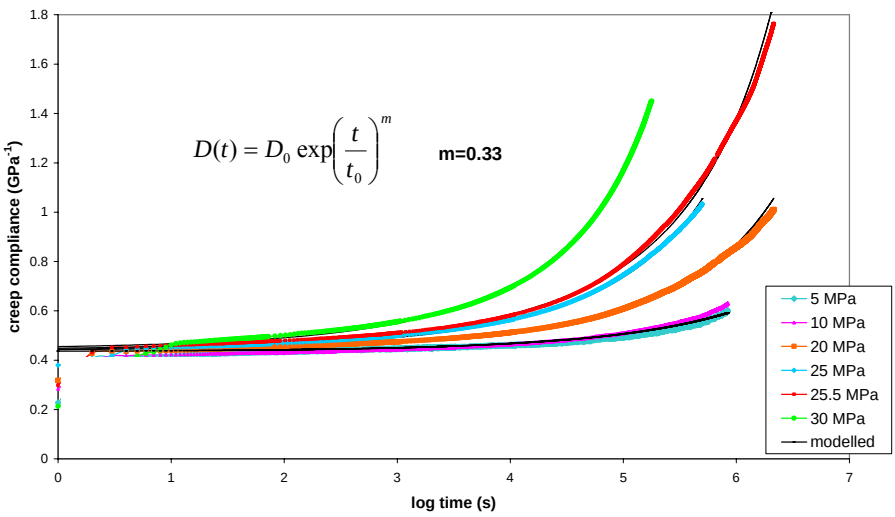

Figure 5.2: Creep compliance curves for DP460 at different levels of stress

The variation of $\mathbf{t_o}$ with $\boldsymbol{\sigma_o}$ can be described with satisfactory accuracy by the empirical relationship:

$$\mathbf{t_o} = \mathbf{A} \exp -\alpha \sigma_o^2 \tag{5.7}$$

The parameters **A** and $\boldsymbol{\alpha}$ can be derived from a linear regression fit to the plot of $\mathbf{log_e}$ $\mathbf{t_o}$ versus $\boldsymbol{\sigma_o}^2$.

Creep behaviour of viscoelastic materials is not only dependent on stress level, but also the stress state[35]. Figure 5.3 clearly shows that there are significant differences in deformation rate with the material deforming more rapidly with time under tension (i.e. reduction in relaxation time $\mathbf{t_o}$ is less under compression than under tension).

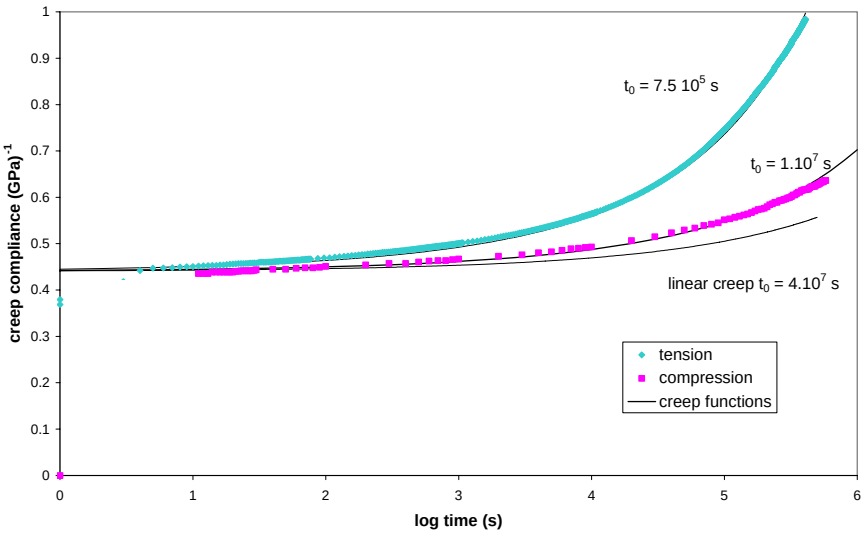

Figure 5.3: Tensile and compressive creep data for DP460 at a stress of 25 MPa (Modelled using different relaxation times t_o)

The results indicate that the stress in Equation (5.7) should be replaced by an effective stress $\bar{\sigma}$ that is a function of both the shear and hydrostatic components of the creep stress. The simplest function to consider is:

$$\bar{\sigma} = \frac{(\lambda+1)}{2\lambda}\,\sigma_e + \frac{3(\lambda-1)}{2\lambda}\,\sigma_m \tag{5.8}$$

where σ_e is the effective shear stress given, in terms of principal components of the applied creep stress, by:

$$\sigma_e = \left[\frac{1}{2}\left[(\sigma_1-\sigma_2)^2 + (\sigma_2-\sigma_3)^2 + (\sigma_1-\sigma_3)^2\right]\right]^{1/2} \tag{5.9}$$

and σ_m is the hydrostatic component of the creep stress given by:

$$\sigma_m = \frac{1}{3}(\sigma_1 + \sigma_2 + \sigma_3) \tag{5.10}$$

σ_1 , σ_2 and σ_3 are the principal stresses and λ is a measure of the sensitivity of the mean creep relaxation time to the hydrostatic component of the stress.
Combining Equations (5.7) and (5.8) gives:

$$t_o = A\exp -\alpha\bar{\sigma}^2 \tag{5.11}$$

Under tensile creep stress σ_o:

$$\sigma_e = \sigma_o \text{ and } \sigma_m = \sigma_o/3 \text{ so } \bar{\sigma} = \sigma_o. \tag{5.12}$$

Under compressive creep stress σ_c:

$$\sigma_e = \sigma_c \text{ and } \sigma_m = -\sigma_c/3 \text{ so } \bar{\sigma} = \frac{1}{\lambda}\sigma_c \tag{5.13}$$

5.2.3 Time-Dependent Plasticity

A generalised creep function used in FEA packages, such as ABAQUS, arising from flow by rate-dependent plasticity takes the form[32]:

$$\dot{\varepsilon}_{ij}(t) = \dot{\varepsilon}_s\left(\frac{\partial\sigma_e}{\partial\sigma_{ij}}\right) + \dot{\varepsilon}_{sw}\,\delta_{ij} \tag{5.14}$$

This expression can be derived from the flow law in a model for deformation by plasticity where the flow potential has contributions from the shear and hydrostatic stress given by the linear Drucker-Prager model[36]:

$$\mathbf{F} = \sigma_e + \mu\sigma_m \tag{5.15}$$

where μ is the flow parameter. The terms $\dot{\varepsilon}_s$ and $\dot{\varepsilon}_{sw}$ can then be associated with contributions to the creep strain rate arising from shear and dilatational (swelling) flow processes.

With reference to Equation (5.14), it can be shown that:

$$\frac{\partial\sigma_e}{\partial\sigma_{ij}} = \frac{3}{2\sigma_e}\left(\sigma_{ij} - \sigma_m\,\delta_{ij}\right) \tag{5.17}$$

Substituting this into Equation (5.14) gives:

$$\dot{\varepsilon}_{ij}(t) = \dot{\varepsilon}_s\,\frac{3\sigma_{ij}}{2\sigma_e} + \left(\dot{\varepsilon}_{sw} - \frac{3\sigma_m}{2\sigma_e}\right)\delta_{ij} \tag{5.18}$$

The creep function for adhesives, Equation (5.4), can be generalised to describe multiaxial creep and takes a form:

$$\dot{\varepsilon}_{ij}(t) = \left((1+\nu)D_o\,\sigma_{ij} - 3\nu\,D_o\,\sigma_m\,\delta_{ij}\right)\frac{m\,t^{m-1}}{t_o^{\,m}}\,\exp\left(\frac{t}{t_o}\right)^m \tag{5.19}$$

where ν is Poisson's ratio assumed to be independent of time, and $\mathbf{t_o}$ is given by Equation (5.11). This can be identified with Equation (5.18) if:

$$\dot{\varepsilon}_s = \frac{2\sigma_e}{3}(1+\nu)\,D_o\,.\,\frac{m}{t_o^{\,m}}\,.\,t^{m-1}\,\exp\left(\frac{t}{t_o}\right)^m \tag{5.20}$$

and

$$\dot{\varepsilon}_{sw} = \frac{\sigma_m\,m}{t_o^{\,m}}\,(1-2\nu)D_o\,t^{m-1}\,\exp\left(\frac{t}{t_o}\right)^m \tag{5.21}$$

where $\mathbf{t_o}$ is a function of σ_e and σ_m given by Equations (5.11) and (5.8).

5.2.4 Physical Ageing

Physical ageing in glassy polymers occurs after the polymer is cooled to temperatures below $\mathbf{T_g}$. At an elevated temperature, where a polymer is in the rubbery state, the structure of the material, as determined by molecular conformations, is in equilibrium. As the temperature is cooled through the glass transition temperature, conformational changes that are needed to maintain an equilibrium structure are restricted by the increase in the relaxation times (reduced mobility) of molecular rearrangements at the

lower temperatures. These non-equilibrium structures have a relatively high mobility to relaxation processes under creep loading, and this gives rise to relatively rapid creep at short elapsed times after cooling.

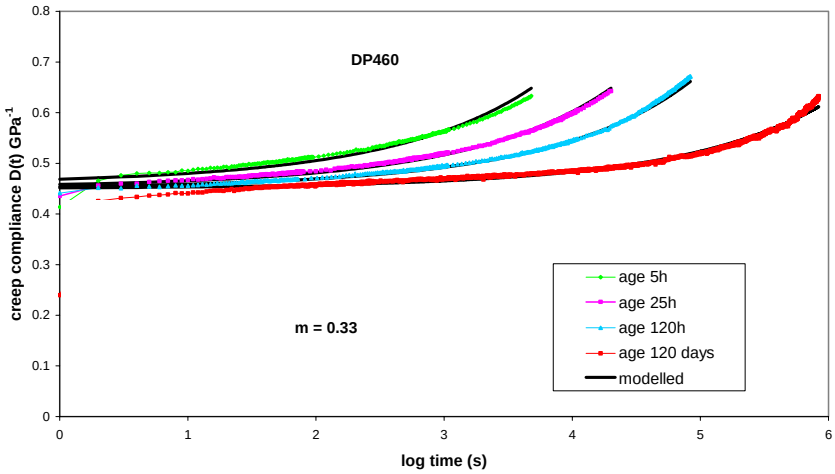

Figure 5.4: Creep compliance curves for DP460 (at σ_o = 6.6 MPa and at different states of physical ageing)

Despite the low temperature of the glassy polymer, there is sufficient molecular mobility for structural changes to take place with subsequent elapsed time (physical ageing) leading to structural states that become progressively closer to equilibrium for the low temperature. These ageing processes give rise to a reduction in molecular mobility under creep and a shift in creep curves to longer creep times as shown in Figure 5.4. The tensile creep behaviour shown in Figure 5.4 can be modelled using Equation (5.5). The continuous lines are best fits to data at each elapsed time. The only parameter to change in each curve is the mean relaxation time $\mathbf{t_o}$. The increase of $\mathbf{t_o}$ with physical age can be expressed by the following equation[34]:

$$\mathbf{t_o = B\, t_e^{\mu}} \tag{5.22}$$

The values of μ and **B** are experimentally derived from creep tests conducted at different ageing times.

5.3 Polymer Composites

Findley's power law model is widely used for describing the viscoelastic behaviour of composite materials under a constant (static) stress. The model has been applied to a range of composite materials and has been included in the ASCE Structural Plastics Design Manual[37]. The time-dependent creep strain $\boldsymbol{\varepsilon(t)}$ is determined using[38]:

$$\boldsymbol{\varepsilon(t) = \varepsilon'_o + \varepsilon'_t t^n} \tag{5.23}$$

where ε'_0 is the stress-dependent and temperature-dependent initial elastic strain, ε'_t is the stress-dependent and temperature-dependent coefficient, **n** is a stress-independent material constant and **t** is the time after loading.

The terms ε'_0 and ε'_t are often expressed as a polynomial series as shown below[38]:

$$\varepsilon'_0(\sigma,T) = a_1\left(\frac{\sigma}{\sigma_0}\right) + a_2\left(\frac{\sigma}{\sigma_0}\right)^2 + a_3\left(\frac{\sigma}{\sigma_0}\right)^3 + \ldots \tag{5.24}$$

$$\varepsilon'_t(\sigma,T) = b_1\left(\frac{\sigma}{\sigma_0}\right) + b_2\left(\frac{\sigma}{\sigma_0}\right)^2 + b_3\left(\frac{\sigma}{\sigma_0}\right)^3 + \ldots \tag{5.25}$$

Equation (5.23) can be rewritten in terms of creep compliance as follows:

$$D(t) = D_0 + D_t t^n \tag{5.26}$$

where **D(t)** is time-dependent creep compliance, σ is stress, D_0 is the instantaneous creep compliance and D_t is the amplitude of transient creep compliance.

Findley's power law can also be used to derive expressions for time-dependent in-plane and through-thickness viscoelastic moduli of composite materials:

$$E_v = \frac{E_0 E_t}{E_t + E_0 t^n} \tag{5.27}$$

where E_v is viscoelastic modulus, E_0 is initial modulus and E_t characterises time dependent behaviour.

When the applied loads are approximately constant for the duration of loading, a "pseudo-elastic" design method may be used. Creep or time-dependent modulus:

$$E(t) = \sigma/\varepsilon(t) \tag{5.28}$$

may be modelled by the following relationship:

$$E(t) = E_o t^{-n} \tag{5.29}$$

E_O is initial (or 1 second) modulus and **n** is the creep index (an experimentally derived constant). The value of E_O is obtained by extrapolation. This approach can be used for different loading modes and elastic properties. The creep index **n** is a measure of viscoelastic behaviour and is dependent on the resin type and degree of cure, fibre format, orientation of the fibres with respect to the applied load, fibre volume content, loading regime and environmental effects (i.e. temperature, moisture and aggressive chemicals). Creep index can be obtained from the gradient of **E(t)** versus **log t** (see Figure 5.5). Low values of **n** can be expected for elastic materials reinforced with continuous aligned fibres. The value of **n** is lower in the fibre direction for these materials. In fact, loading along the fibre direction is unlikely to result in significant

creep deformation. Creep index increases for random fibre formats (e.g. CSM) and unfilled materials. For design purposes, creep modulus and creep index should be obtained direct from experiments on the composite system.

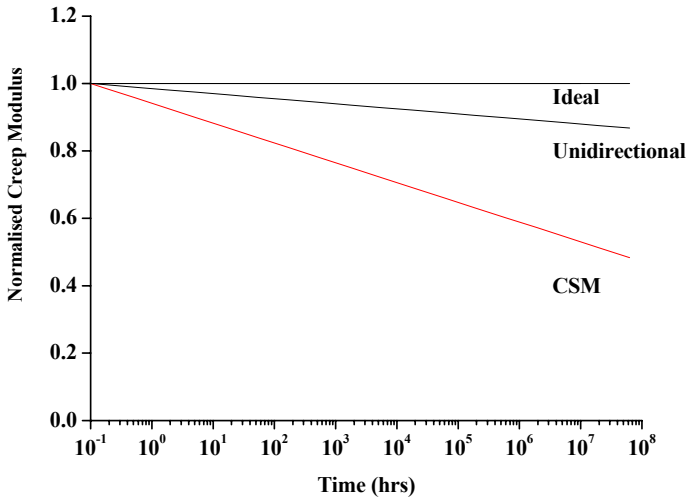

Figure 5.5: Normalised creep modulus for composite materials loaded in tension

6 Life Prediction from Fatigue Behaviour

6.1 Introduction

Fatigue behaviour is usually expressed in terms of the maximum applied fatigue stress **S** and fatigue life (number of cycles to failure $\mathbf{N_f}$). This section examines a number of approaches to predicting fatigue performance of composite laminates (including statistical, fracture mechanics and empirical models)[39].

Constant Amplitude Loading is defined by the following terms:

Minimum stress, σ_{MIN}
Maximum stress, σ_{MAX}
Stress range, $\Delta\sigma = \sigma_{MAX} - \sigma_{MIN}$
Stress amplitude, $\sigma_A = \Delta\sigma/2 = (\sigma_{MAX} - \sigma_{MIN})/2$
Mean stress, $\sigma_{MEAN} = (\sigma_{MAX} + \sigma_{MIN})/2$
Stress ratio, $\mathbf{R} = \sigma_{MIN}/\sigma_{MAX}$
R = –1 for fully reversed loading
R = 0 for zero-tension fatigue, and
R = 1 for a static load.

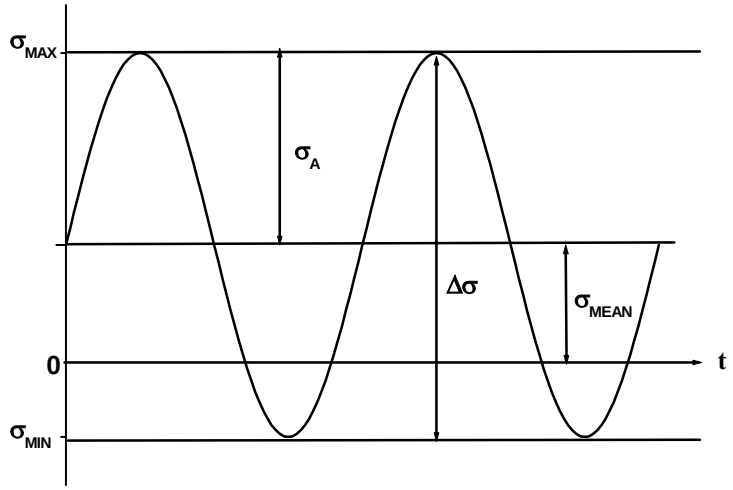

Figure 6.1 Stress parameters for constant amplitude sinusoidal stress-time cyclic loading

6.2 Strength Degradation – Deterministic Approach

The residual strength, **S(N)**, initially equals the static strength σ_{ULT}, and is assumed to monotonically decrease with fatigue cycles. Ignoring environmental and frequency

effects, the rate of degradation should be dependent on σ_{ULT}, the magnitude of the maximum stress σ_{MAX} and the stress ratio **R** ($\sigma_{MIN}/\sigma_{MAX}$).
The residual strength **S(N)** has been written in the form of:

$$S(N) = \sigma_{ULT} - (\sigma_{ULT} - \sigma_{MAX})\left(\frac{N}{N_f}\right)^{v} \qquad (6.1)$$

N is the number of constant amplitude loading cycles before carrying out the residual strength test, N_f is the constant amplitude fatigue life and **v** is the "strength degradation parameter". Failure is assumed to occur when the residual strength **S(N)** is equal to the maximum stress σ_{MAX}. The peak stress σ_{MAX} is usually 50% of σ_{ULT}. Equation (6.1) defines a family of **S(N)** curves for residual strength as a function of fatigue loading cycles prior to strength testing. The path of each curve is dependent on the strength degradation parameter **v** with: (i) linear degradation occurring for $v = 1$; (ii) sudden death behaviour for $v >> 1$; and (iii) rapid initial loss of strength for $v < 1$.

6.3 Strength Degradation - Statistical Approach

Due to the inherent variability in residual strength and life expectancy, the deterministic approach has generally proved inaccurate, necessitating statistical analysis of the data. A widely used approach has been to represent the residual strength and life expectancy by two parameter Weibull functions. Using this approach, the probability of failure for constant amplitude loading (i.e. the probability that the residual strength after **N** cycles is less than the maximum applied stress σ_{MAX}) can been expressed as[40]:

$$P[S(N) \le \sigma_{MAX}] = 1 - \exp\left[-\left(\frac{\sigma_{MAX}}{\sigma_{ULT} - (\sigma_{ULT} - \sigma_{MAX})\left(\frac{N}{N_f}\right)^{v}}\right)^{B_f(N)}\right] \qquad (6.2)$$

$B_f(N)$ is the Weibull shape parameter for residual strength.

At zero cycles, Equation (6.2) should reduce to the static strength Weibull cumulative distribution function, which describes the probability that the initial strength S_O is less than or equal to the maximum stress σ_{MAX}. This function has the following form[40]:

$$P[\sigma_{ULT} \le \sigma_{MAX}] = 1 - \exp\left[-\left(\frac{\sigma_{MAX}}{\sigma^{0}_{ULT}}\right)^{B_S}\right] \qquad (6.3)$$

where B_S is the shape parameter for static strength and σ^{0}_{ULT} is a scaling parameter.

Thus, a required scaling factor seems to be missing from Equation (6.2) and one might expect that $B_f(0) = B_S$. Equation (6.2) predicts that $P[S(N_F) \le \sigma_{MAX}] = 1 - 1/e = 0.632$ as $N \rightarrow N_f$. This is a very peculiar result, as one would expect the probability to have some dependence on material properties. The identified problems relating to the use of

Equation (6.2) seem to arise from substituting the deterministic relation given by Equation (6.1) for the residual strength in place of a required scaling factor.

A relation for the Weibull fatigue life distribution is given by[40]:

$$\mathbf{P\,[\,N_f \le N\,] = 1 - \exp\left[- \left(\frac{N}{N_f^o} \right)^{B_L} \right]} \tag{6.4}$$

where $\mathbf{B_L}$ is the shape parameter for fatigue life and where $\mathbf{N_f^o}$ is a scaling parameter.

Static and fatigue life tests are conducted to obtain $\mathbf{N_f}$ and $\boldsymbol{\sigma_{ULT}}$, the shape parameters $\mathbf{B_f(N)}$, $\mathbf{B_L}$ and $\mathbf{B_S}$, and the scaling factors. The "optimum" value of the strength degradation parameter **v** is obtained by determining the best predictive fit of Equation (6.2) to the experimental data. The scatter in residual strength distributions increases with increasing cycles, and hence the shape parameter decreases.

Talreja[41] has considered the statistics of predicting fatigue failure in composites where the following expression, which can be derived from the Paris type of fatigue crack growth law, is used for the residual strength **S(N)** after the $\mathbf{N^{th}}$ fatigue cycle:

$$\mathbf{S^n(N) = S^n(0) - f(\sigma_{MAX})\,N} \tag{6.5}$$

where **n** is a constant and **f** is some function of the maximum cyclic stress $\boldsymbol{\sigma_{MAX}}$. Equation (6.5) is used to find those values of **X** for which the range $\mathbf{S(0) \le X}$ corresponds to the range of residual strengths $\mathbf{S(N) \le x}$.

The use of the Weibull distribution for the cumulative failure probability $\mathbf{P[S(0) \le X]}$, given by Equation (6.3), then leads to the result:

$$\mathbf{P[\ S(N) \le x\ ] = 1 - \exp\left[- \left(\frac{x^n + f(\sigma_{MAX})\ N}{(\ \sigma_{ULT}^o\ )^n} \right)^{B_s/n} \right]} \tag{6.6}$$

The result given by Equation (6.6) does not involve $\mathbf{N_f}$, contrasting with Equation (6.1). Equation (6.6) predicts that the probability function achieves the value unity when **N** approaches infinity, as to be expected. It is of interest to use the approach of Talreja when using Equation (6.2) for the residual strength, which is first written in the form:

$$\mathbf{S(N) = S(0) \left[1 - \left(\frac{N}{N_f} \right)^{v} \right] + \sigma_{MAX} \left(\frac{N}{N_f} \right)^{v}} \tag{6.7}$$

It then follows that $\mathbf{S(N) \le x}$ whenever:

$$S(0) \leq \frac{\sigma_{ULT} - \sigma_{MAX}\left(\frac{N}{N_f}\right)^{\nu}}{1 - \left(\frac{N}{N_f}\right)^{\nu}} \tag{6.8}$$

On using Equation (6.8) in conjunction with Equation (6.3) it follows that:

$$P[S(N) \leq x] = 1 - \exp\left[- \left\{ \frac{x - \sigma_{MAX}\left(N / N_f\right)^{\nu}}{\sigma^{0}_{ULT}\left[1 - \left(N / N_f\right)^{\nu}\right]} \right\}^{B_s} \right] \tag{6.9}$$

When $\mathbf{N \rightarrow 0}$ the Weibull distribution for static strength is recovered, but when $\mathbf{N \rightarrow N_f}$ the probability tends to unity contrasting sharply with the properties of the result of Equation (6.6). The model based on the use of Equation (6.9) is such that there exists a deterministic life $\mathbf{N_f}$ such that it is certain that all samples in the population will have failed after $\mathbf{N_f}$ cycles have been executed. It is concluded that the better approach is to use Equations (6.5) and (6.6) in preference to Equations (6.1), (6.2) and (6.9).

6.4 Stress Transfer Model

Shear-lag models[39, 42, 43] are being used to predict the damage progression and subsequent elastic property degradation of cross-ply laminates under monotonic and cyclic loading conditions. However, these models are empirical and tend to provide higher residual stiffness values than the experimental results. Dr L N McCartney at NPL has developed a stress transfer model, based on stress intensity factors (strain-energy release rates) for predicting the growth of pre-existing defects, and the effects of fatigue damage on the thermo-mechanical performance of $[0_m/90_n]$ cross-ply laminates. The model predicts ply crack formation in 90° plies and thermo-mechanical degradation in a cross-ply laminate during fatigue loading. An attempt to validate the physics/mechanistic model has shown that the first order approach leads to a conservative estimate of fatigue performance that can be exploited in the design of fatigue resistant composite laminates. It has been possible to predict the degradation of all non-shear properties of the laminate as a function of loading cycles. Details of the model and validation work can be obtained by contacting neil.mccartney@npl.co.uk.

6.5 Fracture Mechanics Theory

A form of the Paris Equation can be used to relate crack growth rate **da/dN** per cycle to the maximum value of the applied strain-energy release-rate $\mathbf{G_{MAX}}$[44, 45]:

$$\frac{da}{dN} = C\left(G_{MAX}\right)^{n} \tag{6.10}$$

where **C** and **n** are material constants. This relationship applies only to the linear portion of the logarithmic-logarithmic plot of $\mathbf{G_{MAX}}$ versus **da/dN** (see Figure 6.2).

Alternatively, the crack growth rate can be expressed as a function of the range of strain-energy release-rate $\mathbf{\Delta G}$ (see Equation (6.6)) by[44, 45]:

$$\frac{da}{dN} = A(\Delta G)^q \tag{6.11}$$

where **A** and **q** are constants.

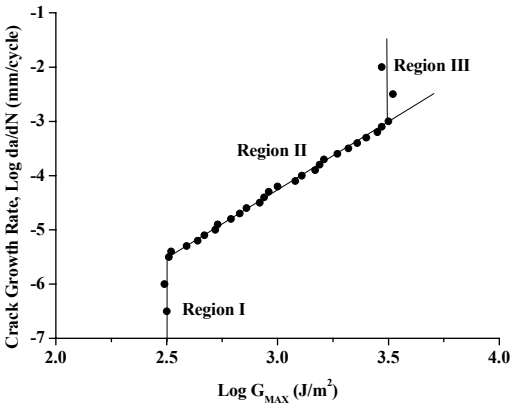

Regions

Region I – Threshold region (G_{TH}) associated with low crack growth rate **da/dN** and G_{MAX} values ($G_{TH} \approx 0.1G_C$).

Region II – Linear region defined by the Paris Law given by Equation (6.4).

Region III – Value of G_{MAX} approaches the adhesive fracture toughness G_c measured under monotonic loading conditions.

Figure 6.2: Typical log-log crack growth rate versus G_{MAX} plot

The difference between maximum and minimum strain-energy release-rate per cycle ΔG is given by:

$$\Delta G = G_{MAX} - G_{MIN} \tag{6.12}$$

This relationship only applies to the linear portion of the logarithmic-logarithmic plot of ΔG versus **da/dN**. Values for both sets of constants (i.e. **C** and **n**, and **A** and **q**) can be determined using linear regression fit to the linear region of the logarithmic-logarithmic plots.

Generally, the relationship between **log** G_{MAX} and **log** ΔG and **log da/dN** is S-shaped (i.e. sigmoidal). This relationship can be described as follows[46, 47]:

$$\frac{da}{dN} = C(G_{MAX})^n \left[\frac{1 - \left(\frac{G_{TH}}{G_{MAX}}\right)^{n_1}}{1 - \left(\frac{G_{MAX}}{G_c}\right)^{n_2}} \right] \tag{6.13}$$

G_{TH} is the minimum (or threshold) value of the adhesive fracture energy, G_c, and **A**, **n**, n_1 and n_2 are material constants. G_c is determined from constant rate of displacement tests (i.e. monotonic fracture energy).

In most practical applications, bonded structures experience mixed-mode loading conditions involving G_I and G_{II} (and in some cases G_{III}) due to the presence of peel and in-plane shear stresses, resulting in mixed-mode cracking. The total strain-energy release-rate G_T (or G_c) is often represented by either a linear interaction or a quadratic relationship:

$$\frac{G_I}{G_{Ic}} + \frac{G_{II}}{G_{IIc}} = 1 \tag{6.14}$$

$$\left(\frac{G_I}{G_{Ic}}\right)^2 + \left(\frac{G_{II}}{G_{IIc}}\right)^2 = 1 \tag{6.15}$$

The equations used to determine the number of fatigue cycles to failure is generally complex. This poses particular problems in applying a fracture mechanics approach to actual structures, particularly where the loading configuration is not a well defined single-mode loading configuration. Design of bonded structures against fatigue using a fracture mechanics approach would require that the maximum fatigue loads be based on $\mathbf{G_{TH}}$ values.

6.6 Empirical Fatigue Theories

There are many empirical fatigue theories that are used to characterise S-N curves for PMCs. A number of these are shown below[48]. It is worth mentioning that these empirical fatigue equations only apply to constant amplitude uniaxial loading conditions and are generally not applicable to in-service situations.

$$\sigma_{ULT} = \sigma_a N^{-m} \tag{6.16}$$

$$\sigma_a = \sigma_{ULT} - b \log N \tag{6.17}$$

$$\sigma_{range} = a + \frac{b}{N^x} \tag{6.18}$$

$$\sigma_{RANGE} = a + \frac{b}{N^x} - \frac{c}{A^y} \tag{6.19}$$

$$A = \frac{1 - R}{1 + R} = \frac{\sigma_{RANGE}}{\sigma_{MEAN}} \tag{6.20}$$

$$R = \frac{\sigma_{MIN}}{\sigma_{MAX}}; \qquad -1 < R \leq 1 \tag{6.21}$$

σ_{MIN} and σ_{MAX} and σ_{MEAN} are the minimum, maximum stresses and mean stresses, respectively for stress cycling. The relations (6.16-6.19) lead to the physically unreasonable situation of unbounded predictions when the number of cycles tends to zero. It would be much more sensible to replace **N** by **N + 1** in these relations, a change that leads to imperceptible differences when applied in a fatigue context.

Harris and co-workers[49,50] have developed a constant life-model (see Equation (6.22)), which according to the authors, agrees well with experimental data for tension-tension, compression-compression and tension-compression fatigue. The model is based on a substantial experimental database including results for different **R** ratios (stress ratio $\mathbf{R} = \sigma_{MIN}/\sigma_{MAX}$), constant and variable amplitude loading, materials (i.e. aramid, carbon and glass fibre-reinforced systems) and lay-ups, etc[51]. The model is

claimed to account for both undamaged and damaged composite materials. Bell-shaped constant life diagrams are used to display the data.

The constant-life model is given by[49-51]:

$$\mathbf{a = f(1-m)^u(c+m)^v} \tag{6.22}$$

where: $\mathbf{a} = \dfrac{\Delta\sigma}{\sigma_{UTS}}$; $\mathbf{m} = \dfrac{\sigma_{MEAN}}{\sigma_{UTS}}$; $\mathbf{c} = \dfrac{\sigma_{UCS}}{\sigma_{UTS}}$

The parameter **c** is the normalised compression strength (i.e. ratio of compressive strength, σ_{UCS}, to tensile strength, σ_{UTS}), **m** is the normalised mean stress component ($\sigma_{MEAN}/\sigma_{UTS}$) and **a** is the normalised stress amplitude ($\Delta\sigma/\sigma_{UTS}$). The parameters **f** (stress function), **u** and **v** in Equation (6.22) are linear functions of **log** $\mathbf{N_f}$.

6.7 Normalised Life Prediction Model

As previously mentioned, the general approach for assessing fatigue performance is to use stress versus number of cycles to failure (**S-N**) curves. These curves enable engineers and designers to determine the fatigue strength (i.e. maximum applied stress σ_{MAX} for given fatigue life $\mathbf{N_f}$). Kawai[52] developed a phenomenological model for determining the off-axis fatigue behaviour of GRP and CFRP laminates. In the model, the fatigue strength is normalised with respect to the ultimate (static) strength σ_{ULT} in the loading direction:

$$\sigma^*_{MAX} = \frac{\sigma_{MAX}}{\sigma_{ULT}} \tag{6.23}$$

For tension-tension and compression-compression fatigue, respectively:

$$\sigma^*_{MAX} = \frac{\sigma_{MAX}}{\sigma_{UTS}} \tag{6.24}$$

$$\sigma^*_{MAX} = \frac{\sigma_{MAX}}{\sigma_{UCS}} \tag{6.25}$$

σ_{UTS} and σ_{UCS} are the ultimate tensile and compressive strengths.

The maximum normalised fatigue stress σ^*_{MAX} is related to the normalised alternating stress σ^*_A and normalised mean stress σ^*_{MEAN} by:

$$\sigma^*_{MAX} = \sigma^*_A + \sigma^*_{MEAN} \tag{6.26}$$

The alternating and mean stresses σ^*_A and σ^*_{MEAN} are defined as:

$$\sigma^*_A = \frac{(1-R)}{2}\sigma^*_{MAX} \tag{6.27}$$

$$\sigma^*_{MEAN} = \frac{(1+R)}{2}\sigma^*_{MAX} \tag{6.28}$$

The above relationships apply within the stress ratio range of $|R| \le 1$.

A new term called the modified non-dimensional effective stress Σ^* is introduced, which is expressed as follows[51]:

$$\Sigma^* = \frac{\sigma^*_A}{1-\sigma^*_{MEAN}} \tag{6.29}$$

This relationship can be rewritten in the following form:

$$\Sigma^* = \frac{\frac{1}{2}(1-R)\sigma^*_{MAX}}{1-\frac{1}{2}(1+R)\sigma^*_{MAX}} \tag{6.30}$$

The evolution of fatigue damage with cycles can be represented by[51]:

$$\frac{d\omega}{dN} = K(\Sigma^*)^{n^*}\left(\frac{1}{1-\omega}\right)^k \tag{6.31}$$

K, $\mathbf{n^*}$ and **k** are material constants.

The effective of frequency on the growth of fatigue damage can be accounted for by considering the rate-dependence of the principal static strengths by which the modified non-dimensional effective stress is normalised. This means that the strength used for normalising data has to be measured at the same effective rate as the fatigue test.

Assuming ultimate failure occurs when ω reaches unity, the fatigue life equation for constant amplitude loading is obtained as:

$$N_f = \frac{1}{(k+1)K(\Sigma^*)^{n^*}} \tag{6.32}$$

Setting $N_f = 1/2$ when $\Sigma^* = 1$, then $(k+1)/K = 2$. This yields the following expression:

$$2N_f = \frac{1}{(\Sigma^*)^{n^*}} \tag{6.33}$$

The master **S-N** relationship obtained by plotting the modified non-dimensional effective stress Σ^* against the number of reversals $2N_f$ to failure on a log-log scale is a straight line.

Equation (6.33) can be rewritten as:

$$\sigma_A^* = \left(\frac{1}{2N_f}\right)^{\frac{1}{n^*}} \left(1 - \sigma_{MEAN}^*\right) \tag{6.34}$$

The normalised constant fatigue life diagram predicted using the above relationship equates to the linear Goodman relation over the stress ratio range $|R| \leq 1$.

Alternatively:

$$\frac{(1-R)\sigma_{MAX}^*}{2-(1+R)\sigma_{MAX}^*} = \left(\frac{1}{2N_f}\right)^{\frac{1}{n^*}} \tag{6.35}$$

For unidirectional E-glass/913 tested at NPL, the value of $\mathbf{n}^*$ is approximately 9.8. A value of $\mathbf{n}^*$ of approximately 10.0 was derived from fatigue tests carried out at NPL on unidirectional E-glass/913. The tests were conducted at three different stress ratios **R** (0.1, 0.5 and 0.75) and at different values of maximum stress σ_{MAX}^* (0.8, 0.7, 0.55, 0.4, 0.25 and 0.2). Not all stress levels were tested for the different ratios. Kawai[51] obtained values of $\mathbf{n}^*$ =14.1 for glass/epoxy and $\mathbf{n}^*$ =11.9 for carbon/epoxy.

Normalised **S-N** curves can be approximated by the following log-linear relationship:

$$\sigma_{MAX} / \sigma_{ULT} = 1 - k \log_{10} N_f \tag{6.36}$$

The gradient of the slope **k** is the fractional loss in strength per decade of cycles and is dependent on the joint geometry and loading conditions. For unidirectional and cross-ply GRP laminates, the value of **k** is ≈ 0.10[50, 52-54]. The corresponding predicted value of **k** is approximately 0.09 using Equation (6.35). Similar behaviour has been observed for a wide range of fibre formats (with and without holes), wet and dry, room temperature and elevated temperatures[54]. The results obtained for unidirectional E-glass/epoxy tested at **R = 0.1** (Figure 6.3) indicate that there may not be a fatigue or endurance limit as previously assumed.

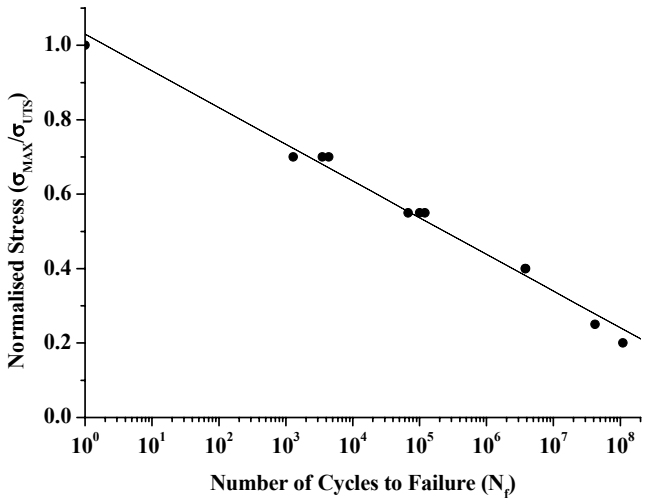

Figure 6.3: Normalised S-N curve for E-glass/epoxy tested at a stress ratio R = 0.1

The relationship between **k** and **R** based on experimental fatigue results for E-glass/913 is (see Figures 6.4 and 6.5):

$$\mathbf{k = 0.104 - 0.047R} \tag{6.37}$$

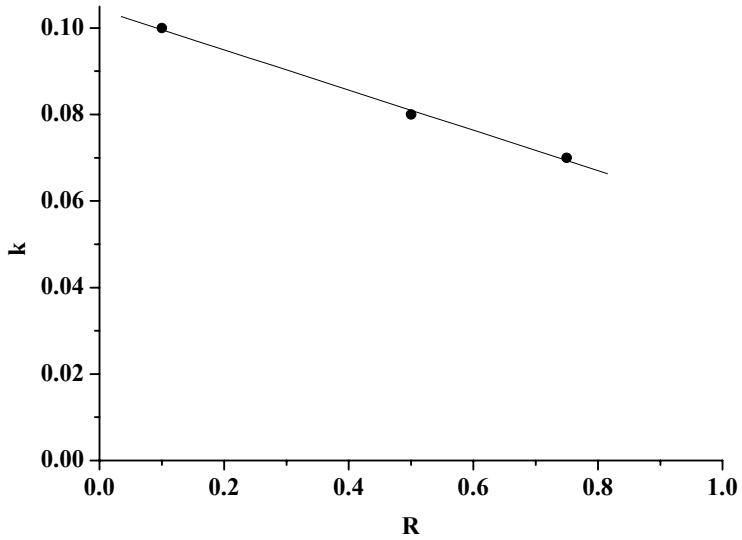

Figure 6.4: Plot of k as a function of R for unidirectional E-glass/epoxy laminates

The predicted relationship between k and R based on Equation (6.35) is:

$$\mathbf{k = 0.095 - 0.053R} \tag{6.38}$$

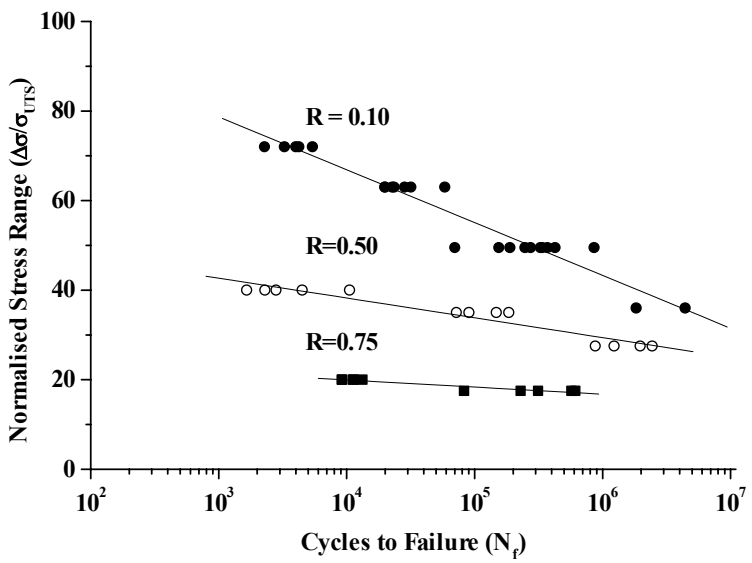

Figure 6.5: S-N curves for unidirectional E-glass/913[50]

7 Standard Accelerated Ageing Test Methods

The following chapter gives an overview of the standard test methods available for conducting accelerated testing of polymers and composites in hostile environments. Comprehensive lists of the ISO and ASTM standards for the accelerated ageing of plastics, rubbers, composites and adhesives are given in appendices 2 and 3.

7.1 Liquid Absorption Test Methods

ISO 175[55] and ASTM D543[56] cover the absorption of chemical liquids into polymers and ISO 62[57] and ASTM D570[58] the absorption of water. In each of these tests standard sized samples are weighed and then immersed at constant temperature in the test liquid. After an agreed time period the samples are removed from the medium and surface liquid wiped off using a dry cloth before weighing. Samples can then be returned to the medium for continuing exposure provided that the time out of the medium is minimised. The balance used should have a resolution of 0.1 mg or better, which can be relaxed to 1 mg if water absorption is greater than 1 %. The increase in mass divided by the initial mass, measured at regular time intervals, is plotted against time in order to define the absorption curve. Results can be reported either as the mass gain after a particular period of immersion or as the mass at saturation defined as the weight gain from 3 successive measurements that differ in value by less than 1% of the overall weight gain.

7.2 Thermal Stability Test Methods

ISO 2578[59] gives a standard procedure for the thermal stability of polymers using the Arrhenius expression. The standard enables the user to define the highest temperature to which a plastic can be subjected for a chosen length of time before a particular property will have degraded unacceptably. The property of the polymer and the level at which it is considered unacceptable will depend on the particular application. The significance of this standard is that it is the only one to specify the Arrhenius method or any other procedure for making long-term prediction from multi-point polymer ageing data.

ISO 176[60] and ASTM D1203[61] cover the stability of plasticisers in polymers, both measuring the amount of plasticisers that is lost due to absorption on activated charcoal. These test methods are both essentially simple quality control tests.

7.3 ESC Test Methods

7.3.1 Introduction

The evaluation of ESC resistance is covered by a number of national and international standards[62]. These test methods can be divided roughly into two groups those that are based on an applied deformation and those based on applied load. The main international standards for testing ESC resistance are:

Constant deformation tests

- Bent strip[63]
- Bent strip test for flexible materials[64]
- Ball and pin impression[65,66]
- Constant tensile deformation[67]
- Slow strain rate testing[68]

Constant load tests

- Constant tensile stress[69]
- C-ring tests[70]

The following section gives a brief overview of the ESC test methods that have been standardised. More detailed information about these and other non-standard test methods can be obtained from a recent technical review on ESC test methods produced by Turnbull and Maxwell[62].

7.3.2 Bent Strip Tests

The bent strip test (ISO 4599)[63] involves clamping the test specimen to a semicircular former to apply a known strain to the specimen. The radius of curvature of former can be varied to induce different levels of stress in the specimen. This strain may be calculated using the following equation:

$$\varepsilon(\%) = \frac{d}{2r + d} \times 100$$

where d is the thickness of the specimen and r is the radius of the former.

Once the specimen has been strained it is brought quickly into contact with the chemical environment. After an agreed time the specimens are removed from the apparatus and either visually inspected for crazing or mechanically tested to assess their residual strength.

This test is most commonly used for assessing the ESC susceptibility of amorphous polymers. It is not suitable for semi-crystalline polymers, which are susceptible to rapid stress relaxation, as the stress applied to the specimen will decrease during the test.

7.3.3 Bent Strip for Flexible Materials

This test was developed by Bell laboratories in the USA and has since been standardised as ASTM D1693[64]. The technique is suitable for flexible polymers such as polyethylene but should only really be used for quality control purposes. An illustration of the type of apparatus used in this test method is shown in Figure 7.1. The specimens used in this test are notched rectangular strips (38 × 13 × 3 mm) that are clamped in a jig so that the sample folds over on itself at an angle of 180° to produce stress within the specimen. Once loaded into the jig the specimens are immediately exposed to the chemical environment at the required test conditions. The specimens are then inspected visually at agreed time intervals and the time required for 50% of the specimens to fail is noted.

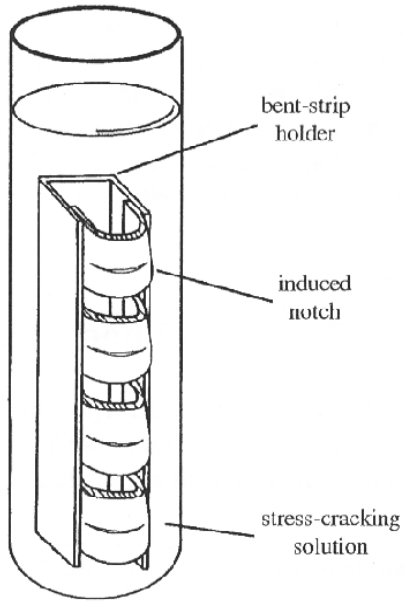

Figure 7.1 Bent strip technique for flexible polymers[64]

7.3.4 Ball and Pin Impression

The ball and pin impression test[65,66] is used primarily for complex finished components. The method involves drilling a series of holes of a specific diameter into the polymer. A series of oversized balls or pins are inserted into the holes to induce a range of different stresses. One hour after the pins have been inserted the specimens are immersed in the environment for 20 hours. The specimens are then dried and visually examined for crazes. The smallest ball to cause visible crazing is used to determine the ESC resistance of the polymer.

7.3.5 Constant Tensile Deformation

The constant tensile deformation test is a relatively new test that is currently being developed as an ISO standard as ISO DIS 22088 part 5[67]. The test method involves applying a constant deformation to the specimen and monitoring the stress relaxation that occurs while it is immersed in the chemical environment. The test is repeated using progressively smaller levels of deformation until the stress relaxation curves of consecutive tests superimpose on one another Figure 7.2. The applied stress required to produce this level of deformation is defined as the critical stress. The ESC resistance of the material is determined by comparing the critical stress obtained in the environment to that obtained in air.

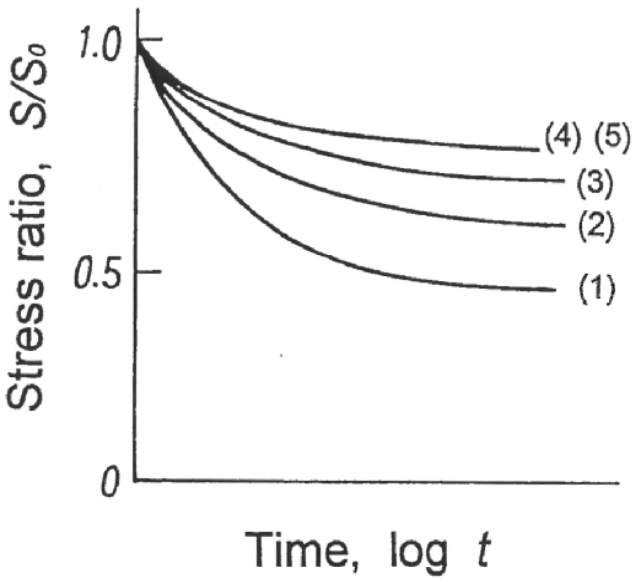

Figure 7.2 Stress relaxation curves obtained using progressively smaller levels of deformation (1>5) until consecutive curves superimpose on one another (4 and 5)[67].

Note: S_0 is the initial stress and S is the stress at time t.

7.3.6 Slow Strain Rate Testing

The slow strain rate method has been used only comparatively recently for characterising the performance of plastics although it is a well established for metals and it is now currently being developed into a standard[68] as ISO DIS 22088 part 6. The test method involves subjecting a specimen to a gradually increasing strain at a constant displacement rate whilst it is exposed to the chemical environment. The tests are conducted under uniaxial tension at low strain rates to enhance the influence of the environment on the specimen. Load and displacement are monitored continuously to enable stress-strain curves to be produced. The development of crazes within the specimen causes the strain to be taken up locally at the crazes such that the stress required to deform the specimen is reduced compared to that in an inert environment. The onset of craze initiation can therefore be detected by the departure of the stress-strain curve in the chemical environment from that in air Figure 7.3. The main advantages of the slow stain rate test are that it is relatively rapid, requires few specimens and can be automated.

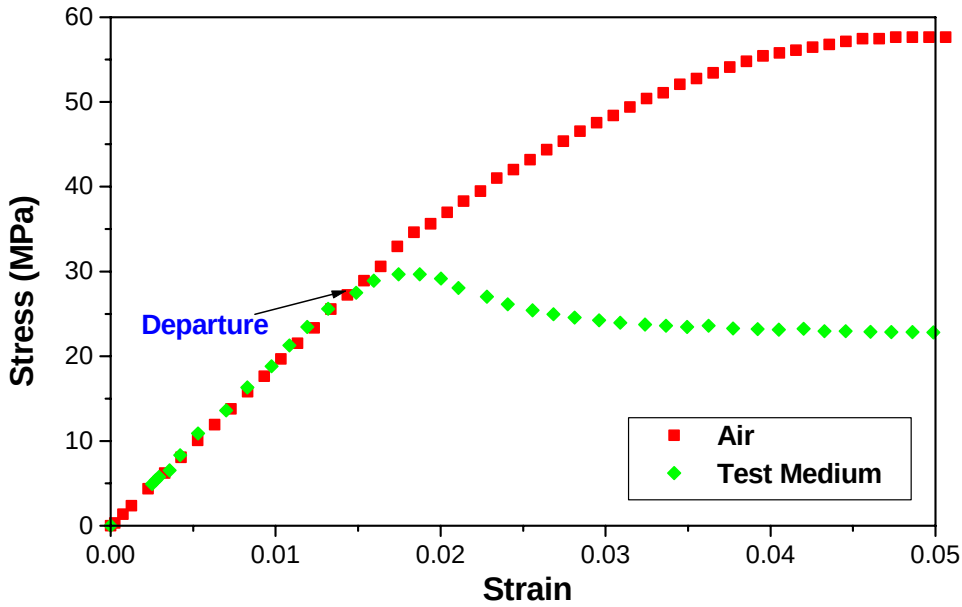

Figure 7.3 Typical stress-strain plot showing difference in stress/strain profile for material exposed in air and in the test medium[68].

7.3.7 Constant Tensile Stress Test

The distinctive feature of this test is that a constant load is applied to the specimens, thereby avoiding the problem of stress relaxation that is found in the constant strain test methods[69]. An illustration of the type of apparatus used in this test method is shown in Figure 7.4. The technique involves subjecting the specimen under investigation to a constant tensile stress at a stress below the tensile yield stress of the polymer. This is usually achieved using a dead weight that is suspended from one end of the specimen. The specimen is then immersed in the stress-cracking agent and inspected at regular intervals to establish the onset of crazing. The time required for crazes/cracks to appear after the specimen has been exposed, or the threshold stress below which no crazes appear in a specific time period (typically 100 hours) can be used as a measure of the ESC resistance.

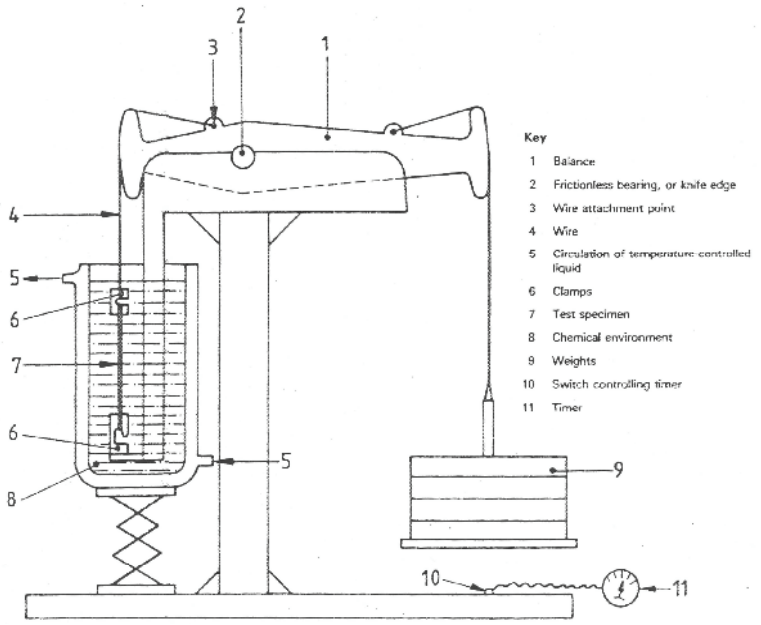

Figure 7.4 Illustration of typical apparatus used for a constant load test[69]

7.3.8 C-ring Tests

C-ring specimens are often used for the testing of tubing and pipe and have been standardised for the testing of polyethylene pipes in ASTM F-1248[70]. Typical apparatus for testing C-ring specimens is shown in Figure 7.5. Circumferential stress is of principle interest and this stress varies around the circumference of the C-ring from zero at each bolthole to a maximum at the outer surface of the middle of the arc opposite the stressing bolt. C-rings can also be stressed in the reverse direction by spreading the ring and creating a tensile stress on the inside surface. An almost constant load can be developed on the C-ring specimen by placing a calibrated spring on the loading bolt.

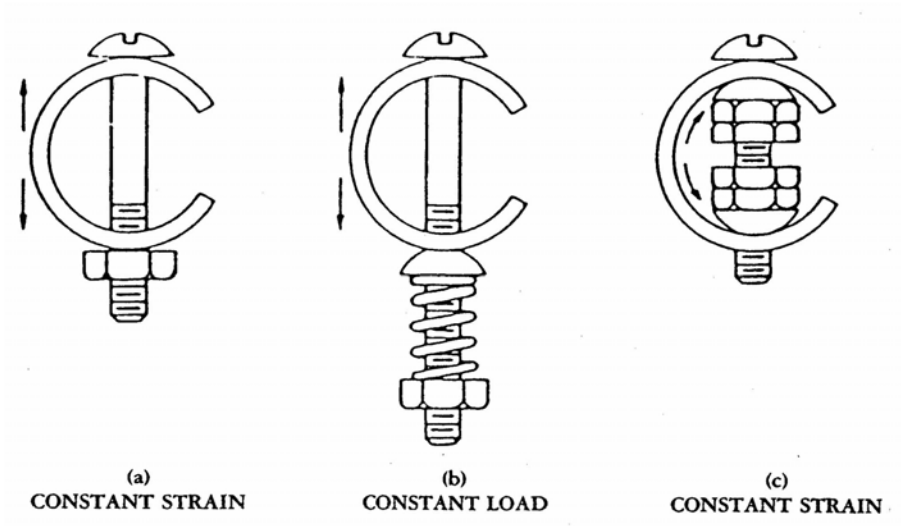

Figure 7.5 C-ring test methods for assess ESC in pipe-sections.

7.4 Weathering Test Methods

7.4.1 Natural Exposure

As the ultimate aim of accelerated ageing is to improve lifetime prediction under service conditions, the most appropriate conditions are those that match the service environment exactly. These are most easily obtained by naturally exposing specimens at outdoor exposure sites. The problem with this is that the exposure period required would have to be at least as long as the life-expectance of the product. Natural weathering is therefore normally accelerated by exposure to climatic conditions that are more severe than those that are expected in service. For this purpose there are a number of established test sites in Saudi Arabia, Australia and the southern states of the USA[71]. Arizona is popular for exposure in hot dry climates and Florida for hot humid climates. Acceleration can also be achieved by the use of Fresnel mirrors[71] that concentrate the sunlight directed on to the specimen.

Standard test procedures for the weathering of polymers in natural daylight, glass-filtered daylight and concentrated sunlight using Fresnal mirrors are given in ISO 877[72], ASTM D1435[73], ASTM D4364-02[74] and ASTM G24-05[75].

7.4.2 Artificial Exposure

Artificial weathering involves exposing test specimens to an artificial light source in a cabinet in which the temperature, humidity and water spray are controlled. The advantage of artificial weathering is that it is easier to accelerate the testing as all of the exposure conditions are controlled. The problem with this approach is to know how these different parameters interact in the weathering process. The key parameter in all accelerated weathering apparatus is the light source, which should ideally simulate solar radiation. The main types of artificial light sources that are used are: carbon-arc, xenon-arc and fluorescent tube[76].

7.4.2.1 Carbon-Arc

Until the 1960's the only light source available with a sufficient radiation levels was the carbon-arc source. A typical spectrum from a carbon-arc consists of a series of line emissions that are superimposed on to a continuous background (Figure 7.6). The spectrum is not a good match for the solar radiation, particularly at the lower wavelengths (<350nm). These high energy, short wavelengths lead to such intensive damage that it bears little relationship to any natural weathering process. In spite of these deficiencies carbon-arc lamps are still in commercial use today and there use for plastics is standardised in ISO 4892: part 4[77] and ASTM D1499-99[78].

7.4.2.2 Xenon Lamps

Xenon-arc lamps give a much better spectral simulation to natural sunlight (Figure 7.7) than other light sources but are considerably more expensive to purchase and maintain. The xenon-arc spectrum contains ultraviolet wavelengths shorter than those found in solar radiation but filters can easily remove these. Xenon lamps also emit high levels of infrared radiation, which must also be removed to prevent overheating of the specimen. Typical xenon exposure equipment such as the Xenon 1200 described by Davis and Sims includes water spray, light/dark cycling and humidity control. Xenon lamps are now considered to be the preferred source where the total solar spectrum is required. Test procedures for the use of xenon lamps have been standardised in ISO 4892: part 2[79] and ASTM D2565-99[80].

7.4.2.3 Fluorescent Tube Lamps

Fluorescent tubes are a considerably cheaper alternative to xenon-arc lamps, capable of simulating the solar spectra in the critical ultraviolet region of the spectra (Figure 7.8). The radiation from a fluorescent lamp is produced by re-emitting the long wavelength spectra from a low-pressure mercury vapour source. This is achieved by a phosphor coating on the inner surface of the bulbs. The spectral distribution of the light radiated by the tubes can vary depending on the type of tube used. For rapid acceleration of the tests UV-B tubes can be used. These have a strong UV peak at around 313 nm, which as a consequence accelerates the degradation process. However, they also transmit intense radiation below 270 nm, which are not found in solar radiation and can lead to degradation not found in normal service. UV-A fluorescent lamps emit radiation at a much higher wavelength producing spectra that are closer to that of solar radiation in the UV region. UVA-340 lamps manufactured by Q-Panel have a UV spectrum (295-350 nm) that is particularly close to that of solar radiation and these are frequently used in weathering studies. Outside the UV region (>350 nm) these lamps do not emit substantial levels of radiation. As most of the degradation processes in polymers occur in the UV region this is not normally a problem. However, this characteristic does have implications for certain polymers. For example substantial degradation occurs in nylon-6 at a wavelength of 365 nm that is not well represented by fluorescent tubes. Wypych[76] gives numerous examples of other high wavelength degradation processes in his book. Standard test procedures for the use of fluorescent tube are given in ISO 4892 part 3[81] and ASTM D4329-99[82].

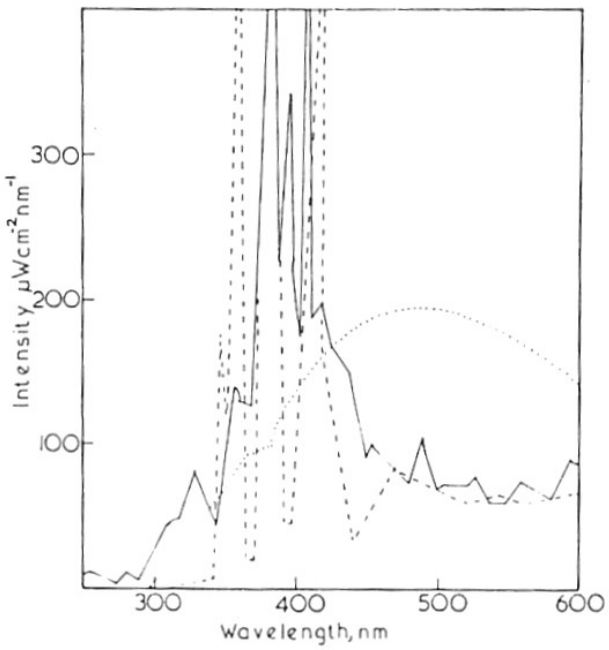

Figure 7.6 Spectrum of carbon-arc lamp (———), carbon-arc lamp with a Cordex D filter (--------) and noonday Chicago sunlight (·····)[76].

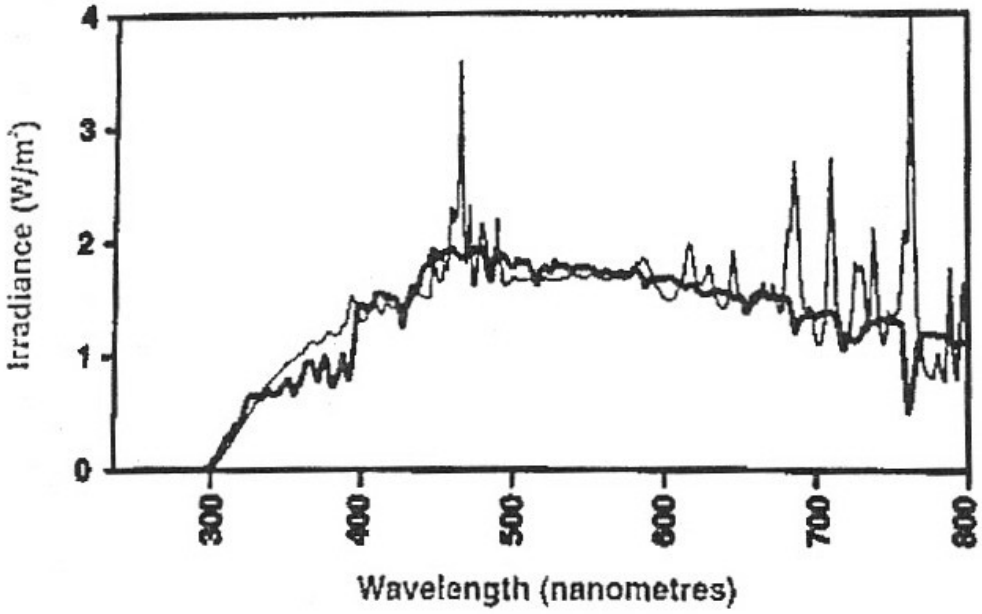

Figure 7.7 Spectrum of a xenon lamp (———) compared with noonday Miami sunlight (———)[76].

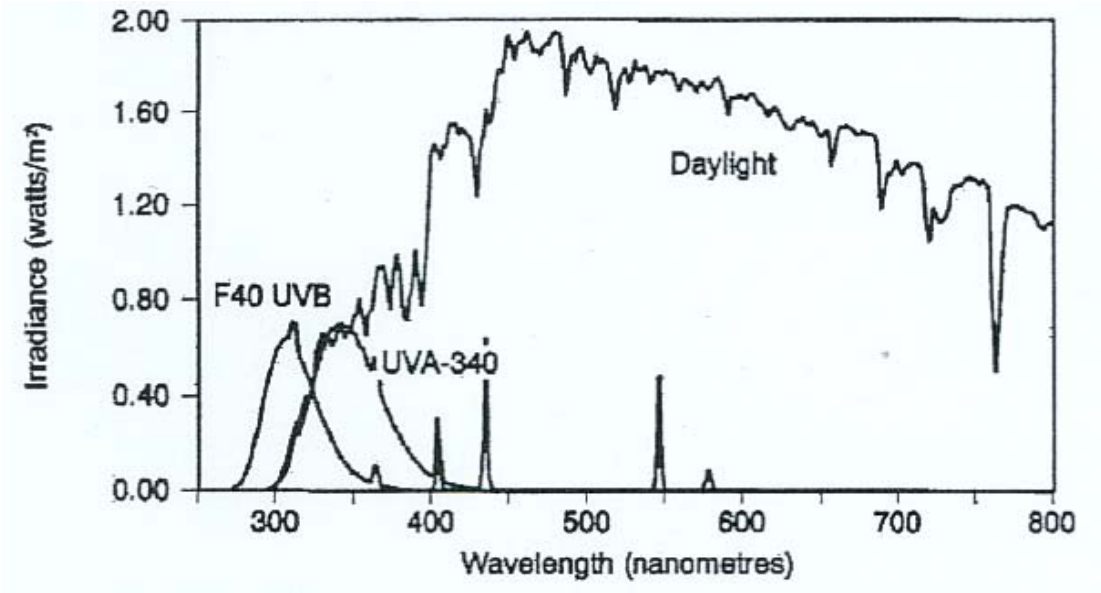

Figure 7.8 Spectra of UV-A and UV-B fluorescent lamps compared to noonday Miami sunlight[76].

7.5 Evaluation of Chemical Resistance of GRP Components

An important aspect for composites in many applications is that these materials are frequently used for their good corrosion resistance (e.g. boats, process equipment, sewage applications). Part 2 of prEN 13121[83] is solely devoted to the determination of chemical resistance as befits a standard on chemical process vessels and aims to provide a partial design factor, A_2, that can be used in the design of a component to take into account the chemical resistance of the material from which it is constructed. Table 7.1 of the standard gives the required thickness for different protective layers, which may be a single protective layer (SPL), a chemically resistant layer (CRL) or one of several thermoplastic linings (TPL).

In accordance with the main philosophy, the design factor A_2 is determined using one of several methods depending on circumstances. Five methods are given for determining the factor:

i. through media lists
ii. resin manufacturer's data
iii. thermoplastic liner manufacturer's data
iv. service experience
v. testing in laboratory/in-situ

It is permissible to use the lowest value, if more than one method is used.

In more detail the methods are:

1. The aggressive environments are divided into Cat 1, 2 and 3 media. There are comprehensive instructions depending on service temperatures, type of lining etc.
2. For materials with a deflection temperature under load (DTUL) 20°C greater than the service temperature, cured according to the manufacturer's instructions, partial factors vary between 1.1 and 1.4, and 1.1 and 1.8, for post cured and non-post cured material, respectively, based on the manufacturer's recommendations.
3. Similar approach for thermoplastic liners when used.
4. For service experience greater than 3 years, the same factor may be used, whereas if it has been inspected after this period and found to be satisfactory a reduction not exceeding 0.1 can be made in the design factor. The same factor can be applied for service experience between 6 months and 3 years if internal inspection is satisfactory.
5. Experimental testing is undertaken using the single-sided exposure arrangement shown in Figure 7.9, where one test plate is in the vapour phase and one in the fluid phase. Assessment is based a standardised ~ 3 mm laminate of fixed weight content made by a prescribed method. The tests are undertaken at the design service temperature for a range of exposure times, such as 1, 4, 8, 16 weeks. It is recommended that four exposure units be employed.

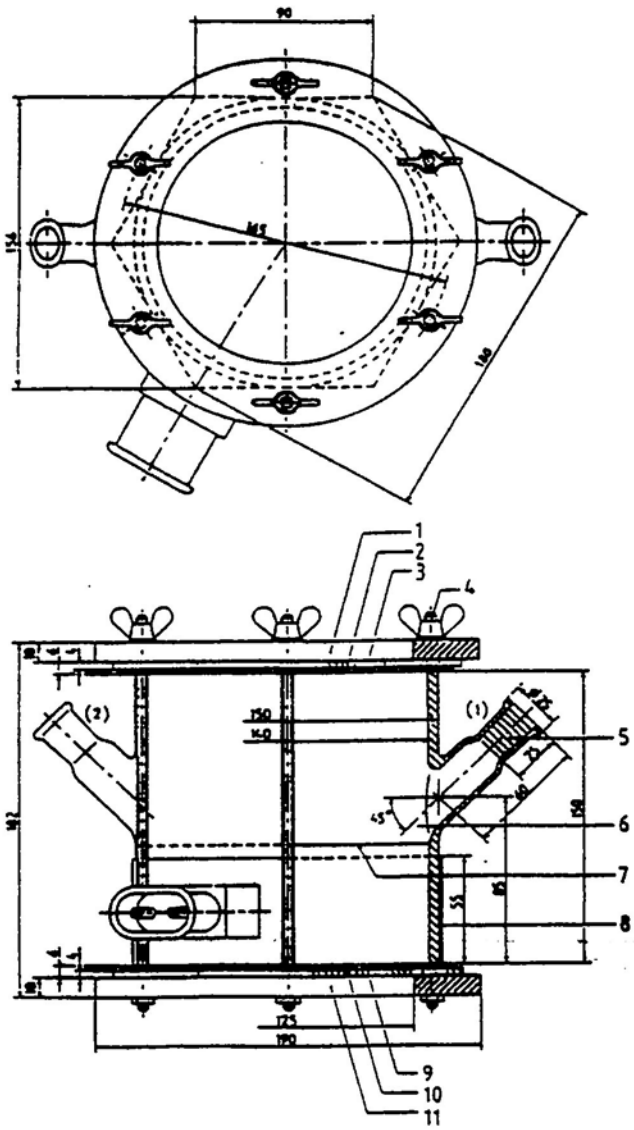

Figure 7.9 Chemical resistance test (n.b. flat plate specimens are numbered 2 and 10)

Degradation is assessed on a combination of appearance changes (10 assessment parameters e.g. gloss), dimensional stability (3 off) and flexural strength/modulus using BS EN ISO 14125[84]. For each property a scoring system is used including a weighting system that increases in order of the above text, with mechanical tests the most important to the final score (see Table 7.1). The flexural properties are plotted as a function of the exposure time and extrapolated to the 50% retention point. If this point is obtained before 10 years, then the material should be rejected for this application (e.g. temperature, concentration etc.). Otherwise, the score varies from zero to 10 based on the percentage loss after 10 years, from 0% to 50%, respectively. Depending on the total score for all aspects, as a percentage of the maximum that could be obtained for the parameters assessed, the partial factor A_2 is obtained from a chart within the range 1.1 to 1.4 (see table 7.2). The weighting factors are different for single-sided and full immersion. The test can be also be conducted by full immersion of 100 mm x 125 mm plates of the laminate or by testing in-situ within a tank.

Table 7.1 Criteria for chemical resistance

Criteria	Weighting factor for single sided exposure	Weighting factor for double sided exposure	Performance level
Appearance			
Colour	2	2	0-5
Gloss retention	3	23	0-5
Opacity	3	3	0-5
Tackiness	4	4	0-5
Fibre prominence	4	4	0-5
Loss of surface resin	5	5	0-5
Blister formation	5	5	0-5
Crazing	5	5	0-5
Crack formation	5	5	0-5
Delamination	5	5	0-5
Dimensional stability			
Swelling	8	4	0-5
Weight change	10	5	0-5
Barcol hardness	5	5	0-5
Mechanical property retention			
Flexural strength	20	10	0-10
Flexural modulus	20	10	0-10

Table 7.2 Determination of partial design factor, A_2

% of total assessment score	A_2
≤ 20	1.1
≤ 30	1.2
≤ 40	1.3
≤ 50	1.4
>50	Unsuitable for purpose

8 Concluding Remarks

A wide range of mechanisms for the degradation of polymers and composites were identified in this review; including thermal degradation, weathering, chemical attack, ESC, ionising radiation, creep and fatigue. Generally there is a good scientific understanding of the mechanisms involved in these degradation processes, but this has not been formalised into procedures or standards. The only standard that could be found that describes how multi-point data can be extrapolated for long-term prediction is ISO 2578, which uses the Arrhenius equation to determine long-term thermal stability. Even in this standard the degree of extrapolation is relatively modest, recommending that results are not extrapolated in time more than a factor of four.

In addition, the wider impact of degradation would appear to be less well understood, in particular the influence that more than one mechanism may have on the overall degradation of the material. For example, specimens weathered in Saudi Arabia often appear to suffer less degradation than specimens artificially weathered in the laboratory. The reason for this apparent discrepancy is that although all the specimens suffer similar ultraviolet damage, the abrasion of desert sands in Saudi Arabia removes the degraded material from the surface of the samples.

Examination of standards revealed that most of the test methods for measuring the degradation of polymers examine a single degradation mechanism in isolation. As demonstrated above this can be misleading. The one exception to this is the standard on the evaluation of chemical resistance in GPR composites, which uses de-rating factors to assess chemical resistance. The main concern with de-rating factors is that their validity in assessing the long-term performance of the material is not always apparent.

The industrial survey conducted by NPL (Appendix 4) attracted responses from a diverse range of companies demonstrating the need for reliable accelerated test methods for polymer-based materials. Although almost half of the correspondents used accelerated test methods very few of them indicated that the test methods had been validated to their satisfaction.

NPL will be continuing this research, included an extensive case study, in this and associated polymer performance projects (Appendix 1). We are therefore keen to obtain further information about issues that are of concern to UK industry and would particularly value any aged specimens or components, where data on the original state of the material is known.

9 Acknowledgements

This work was funded by the DTI National Measurements Systems Directorate under Project F04 of the Measurements for Materials Performance programme.

10 References

1. D.C. Wright, 'Failure of Plastics and Rubber Products – Causes, Effects and Case Studies involving Degradation', Rapra Technology Report, 2001, ISBN: 1-85857-261-8.
2. R.P. Brown, D. Kockott, P. Trubiroha, W. Ketola and J. Shorthouse, 'A Review of Accelerated Durability Tests', VAMAS Report No.18, Edited by R.P. Brown, Versailles Project on Advanced Materials and Standards, 1995.
3. R.P. Brown and J.H. Greenwood, 'Practical Guide to the Assessment of the Useful Life of Plastics', Rapra Technology Limited, 2002.
4. J.R. White and A Turnbull, "Review: Weathering of polymers: mechanisms of degradation and stabilization, testing strategies and modelling", J. Mat. Sci., 29, 584-613, 1994.
5. G. wypych, "Handbook of Materials Weathering", ChemTec publishing, 2003.
6. J.H. Greewnood, 'Life prediction in polymers', ERA Technology Report No. 97-0782R, 1997.
7. D.C. Wright, *Environmental Stress Cracking of Plastics*, Rapra Technology Ltd., 1996.
8. J.C. Arnold, 'Environmental stress crack initiation in glassy polymers', *Trends in Polymer Sci.,* 1996, 4, 403-408.
9. S Wellinghoff and E Baer, 'The mechanism of crazing in polystyrene', *J. Macromol. Sci. B,* 1975, 11(3), 367-387.
10. H.H. Kausch and C. Oudet, 'Progress and challenge in polymer crazing and fatigue', *Makrol. Chem, Macromol. Symp.*, 1988, 22, 207-224.
11. D.C. Wright and K.V. Gotham, 'Solvent crazing criteria', *Polymer Eng. Sci.,* 1983, 23 (3) 135-139.
12. D.C. Wright, 'An inelastic deformation criterion for delayed failure,' *Brit. Polymer J.,* 1978, 10, 60-64.
13. Carfago and Gibson, 'A review of equipment ageing theory and technology', EPRI NP-1558, Electric Power Research Institute, Palo Alto, CA, USA, September 1980.
14. V. Gueguen, L. Audouin, B. Pinel and J. Verdu, 'Polymer Degradation and Stability', 1994, 46(1), 113
15. G.W. Ehrenstein, A Schmiemann, A. Bledzki and R. Spaude, 'Corrosion Phenomena in Glass-Fiber-Reinforced Thermosetting Resins', Volume 1, *Handbook of Ceramics and Composites*, N.P. Cheremisinoff, ed., Marcel Dekker, Inc., 1990.
16. W.R. Broughton, M.J. Lodeiro and S. Maudgal, 'Accelerated Test Methods for Assessing Environmental Degradation of Composite Laminates', NPL Report MATC(A)251, 2000.
17. G. Pritchard, ed., 'Reinforced Plastics Durability', Woodhead Publishing Ltd, 1995.
18. C.S. Smith, 'Design of Marine Structures in Composite Materials', Elsevier Applied Science, 1990.
19. G.D. Sims and W.R. Broughton, Chapter 5, Volume 2, Comprehensive Composite Materials, Edited by A. Kelly and C.H. Zweben, Elsevier, 2000.

20. I. Ghorbel and P. Spiteri, 'Durability of Closed-End Pressurized GRP Pipes under Hygrothermal Conditions. Part I: Monotonic Tests', Journal of Composite Materials", 30(14), 1996, pp 1562-1580.
21. D.W. Levi, R.F. Wegman, M.C., Ross and E.A. Garnis, 'Use of Hot Water Aging for Estimating Lifetimes of Adhesive Bonds to Aluminium', SAMPE Quarterly, 7(3), 1976, pp 1-4.
22. C.C Chamis and P.L.N. Murthy, 'Simplified Procedures for Designing Bonded Composite Joints', Journal of Reinforced Plastics and Composites, Volume 10, 1991, pp 29-41.
23. W.R. Broughton, 'Analytical Models for Assessing Environmental Degradation of Unidirectional and Cross-Ply Laminates', NPL Report MATC(A)1, 2001.
24. G.S. Springer, Editor, 'Environmental Effects on Composite Materials, Volume 1, Technomic Publishing Company, 1984.
25. P.B. Bowden and S. Raha, 'A Molecular Model for Yield and Flow in Amorphous Glassy Polymers Making Use of a Dislocation Analogue', Philosophical Magazine 29, pp 149-166, 1974.
26. M. Kittagawa, 'Power Law Relationship between Yield Stress and Shear Modulus for Glassy Polymers', Journal of Polymer Science: Polymer Physics Edition, Volume 15, pp 1601-1611, 1977.
27. W.R. Broughton, 'Shear Properties of Unidirectional Carbon Fibre Composites, PhD Thesis, Department of Materials Science and Metallurgy, University of Cambridge, Cambridge, United Kingdom, 1990.
28. K.T. Gillen and R.L. Clough, Polym. Degrad. Stab., 24, (1989) 137.
29. K.T. Gillen and R.L. Clough, Polym.Mater. Sci. Eng. 52, (1985) 586.
30. S.G. Burnay, OPERA 89 Conference, Lyon, France, 2, (1999) 561.
31. IEC 61244-2, determination of long-term radiation ageing in polymers – Part 2: Procedures for predicting ageing at low dose rates, 1996.
32. G. Dean and R. Mera, 'Modelling Creep in Toughened Adhesives for Finite Element Analysis', NPL Report DEPC-MPR 003, 2004.
33. L.C.E. Struik, 'Physical Ageing in Amorphous Polymers and Other Materials', Elsevier, Amsterdam, 1978.
34. P.E. Tomlins B.E. Read, 'Creep and Physical Ageing of Polypropylene: A Comparison of Models', Polymer, Volume 39, Number 2, 1998, pp 355-367.
35. G.D. Dean, P.E. Tomlins and B.E. Read, 'A Model for Non-Linear Creep and Physical Ageing in PVC', NPL Report DMM(A)191, 1993.
36. G. Dean and L. Crocker, 'The Use of Finite Element Methods for Design with Adhesives', NPL Measurement Good Practice Guide No 48, 2001.
37. 'Structural Plastics Design Manual', American Society of Civil Engineers, ASCE Publications, 1984.
38. D.W. Scott, J.S. Lai, J.S. and A-H. Zureick, 'Creep Behaviour of Fiber-Reinforced Polymeric Composites: A Review of the Technical Literature', Journal of Reinforced Plastics and Composites, Volume 14, 1995, pp 588-617.
39. B. Harris, Ed., 'Fatigue in Composites', CRC Press, Woodhead Publishing Limited, 2003.
40. J.R. Schaff and B.D. Davidson, 'Life Prediction Methodology for Composite Structures. Part I - Constant Amplitude and Two-Stress Level Fatigue', Journal of Composite Materials", Volume 31, Number 2, 1997, pp 128-157.
41. R. Talreja, 'Fatigue of Composite Materials', Technomic Publishing Company, 1987.

42. W.R. Broughton, 'Analytical Models for Assessing Environmental Degradation of Unidrectional Degradation of Unidirectional Laminates', NPL Report MATC(A)1, 2001.
43. L.N. McCartney, 'Physically Based Damage Models for Laminated Composites'. Proceedings of the Institution of Mechanical Engineers, Volume 217, Part L: Journal of Materials: Design and Applications, 2003, 163-199.
44. A.J. Kinloch and S.O. Osiyemi, 'Predicting Fatigue Life of Adhesively-Bonded Joints', Journal of Adhesion, Volume 43, 1993, pp 79-90.
45. A.J. Curley, H. Hadavinia, A.J. Kinloch and A.C. Taylor, A.C., 'Predicting the Service-Life of Adhesively-Bonded Joints', International Journal of Fracture, Volume 103, 2000, pp 41-69.
46. G. Fernlund, M. Papini, D. McCammond and J.K. Spelt, 'Fracture Load Predictions for Adhesive Joints', Composites Science and Technology, Volume 51, 1994, pp 587-600.
47. I.A. Ashcroft, R.B. Gilmore and S.J. Shaw, 'Cyclic Fatigue and Environmental Effects with Adhesively Bonded Joints', AGARD 83rd SMP Meeting, Florence, 1996.
48. R. Talreja, 'Statisticals Considerations', Chapter 11, 'Fatigue of Composite Materials', K.L. Reifsnider, Ed., Elsevier Science Publishers, 1990.
49. P.T. Curtis, 'Designing for Fatigue and Environmental Effects in Polymer Composites', "International Conference on Designing Cost-Effective Composites, IMechE Conference Transactions, London, UK, 1998, pp 53-63.
50. W.R. Broughton and M.J. Lodeiro, 'Fatigue Testing of Composite Laminates', NPL Report CMMT(A)252, 2000.
51. M. Kawai, 'A Phenomenological Model for Off-Axis Fatigue of Unidirectional Polymer Matrix Composites Under Different Stress Ratios', Composites Part A: Applied Science and Manufacturing, Volume 35, 2004, pp 955-963.
52. G.D Sims and D.G. Gladman, 'Effect of Test Conditions on the Fatigue of a Glass-Fabric Laminate: Part A- Frequency', Plastics and Rubber: Materials and Applications, May 1978, pp 41-48.
53. G.D Sims and D.G. Gladman, 'Effect of Test Conditions on the Fatigue of a Glass-Fabric Laminate: Part B- Specimen Condition', Plastics and Rubber: Materials and Applications, August 1980, pp 122-128.
54. J.F. Mandell, D.D. Huang and F.T. McGarry, 'Tensile Fatigue Performance of Glass-Fiber-Dominated Composites', Composites Technology Review, Volume 3, Number 3, 1981, pp 96-102.
55. ISO 175: 1999, Plastics - Methods of test for the determination of the effects of immersion in liquid chemicals
56. ASTM D543-95 (2001) Standard Practices for Evaluating the Resistance of Plastics to Chemical Reagents
57. ISO 62: 1999, Plastics - Determination of water absorption
58. ASTM D570-98 Standard Test Method for Water Absorption of Plastics
59. ISO 2578 (1993) Plastics -- Determination of time-temperature limits after prolonged exposure to heat
60. ISO 176 (2005) Determination of Loss of Plasticisers - Activated Carbon Method
61. ASTM D1203-94 (2003) Standard Test Methods for Volatile Loss From Plastics Using Activated Carbon Methods
62. A. Turnbull and A.S. Maxwell, '*Test methods for environment stress cracking of polymeric materials*', NPL Technical Review No. 3, (1999)

63. ISO 4599: 1986, Plastics - Determination of resistance to environmental stress cracking (ESC) - Bent strip method.
64. ASTM D 1693-01, Environmental Stress-Cracking of Ethylene Plastics, American Society for Testing of Materials, Phil., USA, (2001)
65. ISO 4600: 1992, Determination of environmental stress cracking (ESC) by the ball or pin impression method.
66. DIN 53449: 1992, Evaluation of Resistance of Thermoplastics to Environmental Stress Cracking, Steel Ball Impression Method.
67. ISO DIS 22088-5: 2004, Plastics – Determination of resistance to environmental stress cracking (ESC) – Part 5: Constant tensile deformation method
68. ISO DIS 22088-6: 2004, Plastics – Determination of resistance to environmental stress cracking (ESC) – Part 6: Slow strain rate method
69. ISO 6252: 1992, Determination of Environmental Stress Cracking (ESC) by the constant tensile stress method.
70. ASTM F1248-96 (2002) Standard Test Method for Determination of Environmental Stress Crack Resistance (ESCR) of Polyethylene Pipe
71. A. Davis and D. Sims, "*Weathering of Polymers*" Applied Science, London, (1983)
72. ISO 877: 1994, Plastics - Methods of exposure to direct weathering, to weathering using glass-filtered daylight, and to intensified weathering by daylight using Fresnel mirrors
73. ASTM D1435-99 Standard Practice for Outdoor Weathering of Plastics
74. ASTM D4364-02 Standard Practice for Performing Outdoor Accelerated Weathering Tests of Plastics Using Concentrated Sunlight
75. ASTM G24-05 Standard Practice for Conducting Exposures to Daylight Filtered Through Glass
76. G. Wypych, *Weathering of Plastics, Testing to Mirror Real Life Performance*, pg 1-13, Plastic Design Library, New York (1999)
77. ISO 4892 Part 4: 2004, Plastics - Methods of exposure to laboratory light sources - Part 4: Open-flame carbon-arc lamps
78. ASTM D1499-99 Standard Practice Filtered Open-Flame Carbon-Arc Type Exposures of Plastics
79. ISO 4892 part 2: 2004, Plastics - Methods of exposure to laboratory light sources - Part 2: Xenon-arc sources
80. ASTM D2565-99 Standard Practice for Xenon Arc Exposure of Plastics Intended for Outdoor Applications
81. ISO 4892 part 3: 2004, Plastics - Methods of exposure to laboratory light sources - Part 3: Fluorescent UV lamps
82. ASTM D4329-99 Standard Practice for Fluorescent UV Exposure of Plastics
83. BS EN 13121-2:2003 GRP tanks and vessels for use above ground. Composite materials. Chemical resistance
84. BS EN ISO 14125:1998 Fibre-reinforced plastic composites. Determination of flexural properties

Appendix 1 Performance Projects and F4 Case Study

The full suite of polymer related projects within the Performance programme are:

B3 A Tool to Predict the Lifetime of Composites
F2 Sensing the Onset of Damage at Polymer Surfaces Due to Environmental Exposure
F4 Accelerated Ageing Protocol For Service in Hostile Conditions
F7 Permeation, Absorption and Desorption of Liquids and Gases in Polymer and Multilayer Systems
F9 Prediction of the Lifetime of Adhesive Joints Under Sustained Loading
F10 Adhesive Design Toolkit
F12 Development of Test Methods for Determining the Criticality of Defects in Composite Materials Systems Under Long-term Loading
G5 Performance of Conformal Coatings in Corrosion Protectioin of Electronic Assemblies

The essential aspects of the case study are outlined below.

- As a main case study the requirements of CEN TC249/SC2/WG6 (convened by NPL) whom are unable to progress their specification standard, EN 13706, for pultruded profiles due to a lack of confidence in the relationship between laboratory data and service life will be used. This will provide validation of experimental procedures for testing programmes as part of the integration with the predictive approaches developed in Task 1.
- Three levels of environment identified that encompass the application areas. These are:
    1. Weathering / No load
    2. Occasional chemical exposure / No load
    3. Full chemical exposure/ Loaded.
- Advantage will be taken of techniques being developed in associated projects such as F2 and F7, to make repeat measurement for this system. The measured data will in turn be feed back to F2 and F7.

Appendix 2 ISO Standards

A2.1 Plastics

Thermal degradation

ISO 176	Determination of Loss of Plasticisers - Activated Carbon Method
ISO 177	Plastics - Determination of Migration of Plasticiser
ISO 291	Plastics - Standard atmospheres for conditioning and testing.
ISO 305	Determination of Thermal Stability of Polyvinyl Chloride Related Chlorine Containing Polymers, and their Compounds - Discoloration Method
ISO 554	Standard atmospheres for conditioning and/or testing - specification.
ISO 1137	Plastics: Determination of Behaviour in a Ventilated Tubular Oven
ISO 1599	Cellulose Acetate- Determination of Viscosity
ISO 2578	Plastics: Determination of Time/Temperature Limits after Exposure to Prolonged Action of Heat
ISO 3671	Determination of Volatile Matter of Amino-plastics Moulding Materials
ISO 3205	Preferred Test Temperatures

Environmental stress cracking

ISO 4599	Plastics - Determination of Resistance to Environmental Stress Cracking (ESC) - Bent Strip Method
ISO 4600	Plastics - Determination of Environmental Stress Cracking (ESC) - Ball and Pin
ISO 6252	Plastics - Determination of Resistance to Environmental Stress Cracking (ESC) - Constant Tensile Stress Method
ISO DIS 22088: Part 5	Plastics - Determination of resistance to environmental stress cracking (ESC) – Constant tensile deformation method
ISO DIS 22088: Part 6	Plastics - Determination of resistance to environmental stress cracking (ESC) – Slow strain rate method

ISO 16770	Plastics - Determination of environmental stress cracking (ESC) of polyethylene -- Full-notch creep test (FNCT)

Effect of liquids

ISO 62	Plastics - Determination of Water Absorption
ISO 175	Plastics - Determining the Effect of Liquid Chemical Including Water
ISO 483	Plastics - Small enclosures for conditioning and testing using aqueous solutions to maintain relative humidity at constant value.
ISO 4611	Plastics - Determination of the Effect of Exposure to Damp Heat, Water Spray and Salt

Weathering

ISO 877	Plastics - Determination of Resistance to Change upon Exposure under Glass to Daylight
ISO 2579	Plastics - Instrumental Evaluation of Colour Differences
ISO 3557	Plastics - Recommended Practice for Spectrophotometry and Calculation of Colour in CIE Systems
ISO 3558	Plastics - Assessment of the Colour of Near-White or Near-Colourless Materials
ISO 4582	Plastics - Determination of Changes in Colour and Variations in Properties and Exposure to Daylight under Glass, Natural Weathering of
ISO 4607	Plastics - Methods of Exposure to Natural Weathering
ISO 4892	Plastics - Methods of Exposure to Laboratory Light Sources
ISO 9370	Guide for the instrumental determination of radiant exposure in weathering tests
ISO TR 9673	Solar radiation and its measurements for determining outdoor weather exposure levels
ISO 11403 Part 3	Environmental influences on properties

Biological attack

ISO 846	Determination of Behaviour under the Action of Fungi and Bacteria - Evaluation by Visual Examination or Measurement of Change in Mass or Physical Properties

Mechanical (Creep)

ISO 899	Plastics -- Determination of creep behaviour

A2.2 Rubbers

Thermal degradation

ISO 188		Accelerated Ageing or Heat Resistance Tests
ISO 6914		Determination of Ageing Characteristics by Measurement of Stress at a Given Elongation

Effect of liquids

ISO 1817		Determination of the Effect of Liquids

Weathering

ISO 4665	Part 1	Assessment of Change in Properties after Exposure to Natural Weathering or Artificial Light
ISO 4665	Part 2	Methods of Exposure to Natural Weathering
ISO 4665	Part 3	Methods of Exposure to Artificial Weathering

Effect of ozone

ISO 1431	Part 1	Resistance of Ozone Cracking - Static Strain Test
	Part 2	Resistance to Ozone Cracking - Dynamic Strain Test
	Part 3	Determination of Ozone Concentration

Biological degradation

ISO 846	Determination of Behaviour under the Action of Fungi and Bacteria - Evaluation by Visual Examination or Measurement of Change in Mass or Physical Properties

Mechanical (Stress relaxation in compression)

ISO 3384	Determination of Stress Relaxation in Compression at Normal and High Temperatures
ISO 6056	Determination of Compression Stress Relaxation (Rings)

A2.3 Composites

ISO 75 part 3	Plastics - Determination of temperature of deflection under load. -- Part 3: High-strength thermosetting laminates and long-fibre-reinforced plastics
BS EN 2378	Fibre reinforced plastics - Determination of water absorption by immersion in demineralised water.
BS EN 2489	Fibre reinforced plastics - Determination of the action of liquid chemicals.
BS EN 2823	Fibre reinforced plastics - Determination of the effect of exposure to humid atmosphere on physical and mechanical characteristics.
ISO 899	Determination of creep behaviour
ISO 13003	Fibre-reinforced plastics -- Determination of fatigue properties under cyclic loading conditions

Note: The standards listed in section A2.3 refer specifically to fibre-reinforced composites. More general standards covering both plastics and composites are given in section A2.1.

A2.4 Adhesives

ISO 9142	Adhesives - Guide to the selection of standard laboratory ageing conditions for testing bonded joints
ISO 9664	Test Methods for fatigue properties of structural adhesives in tensile shear
ISO 10354	Adhesives - Characterisation of durability of structural adhesive assemblies - wedge rupture test
ISO 10363	Hot melt adhesives - Determination of thermal stability
ISO 9142	Adhesives - Guide to the selection of standard laboratory ageing conditions for testing bonded joints
ISO 14615	Adhesives - Durability of structural adhesive joints - Exposure to humidity and temperature under load

Appendix 3 ASTM Standards

A3.1 Plastics

Thermal degradation

D1203-94 (2003)	Standard Test Methods for Volatile Loss From Plastics Using Activated Carbon Methods
D2115-04	Standard Practice for Oven Heat Stability of Poly(Vinyl Chloride) Compositions
D3045-92 (2003)	Standard Practice for Heat Aging of Plastics Without Load

Effect of liquids

D543-95 (2001)	Standard Practices for Evaluating the Resistance of Plastics to Chemical Reagents
D570-98	Standard Test Method for Water Absorption of Plastics
D1712-03	Standard Practice for Resistance of Plastics to Sulfide Staining

Environmental stress cracking

D1693-01	Standard Test Method for Environmental Stress-Cracking of Ethylene Plastics
F1248-96 (2002)	Standard Test Method for Determination of Environmental Stress Crack Resistance (ESCR) of Polyethylene Pipe

Weathering

D1435-99	Standard Practice for Outdoor Weathering of Plastics
D1499-99	Standard Practice Filtered Open-Flame Carbon-Arc Type Exposures of Plastics
D2565-99	Standard Practice for Xenon Arc Exposure of Plastics Intended for Outdoor Applications
D4329-99	Standard Practice for Fluorescent UV Exposure of Plastics
D4364-02	Standard Practice for Performing Outdoor Accelerated Weathering Tests of Plastics Using Concentrated Sunlight

G24-05	Standard Practice for Conducting Exposures to Daylight Filtered Through Glass
G156-02	Standard Practice for Selecting and Characterizing Weathering Reference Materials Used to Monitor Consistency of Conditions in an Exposure Test
G178-03	Standard Practice for Determining the Activation Spectrum of a Material (Wavelength Sensitivity to an Exposure Source) Using the Sharp Cut-On Filter or Spectrographic Technique

Biological attack

G21-96 (2002)	Standard Practice for Determining Resistance of Synthetic Polymeric Materials to Fungi

Mechanical (Creep)

D2990-01	Standard Test Methods for Tensile, Compressive, and Flexural Creep and Creep-Rupture of Plastics

A3.2 Rubber

Thermal degradation

D573-04	Standard Test Method for Rubber—Deterioration in an Air Oven
D865-99	Standard Test Method for Rubber-Deterioration by Heating in Air (Test Tube Enclosure)
D572-04	Standard Test Method for Rubber—Deterioration by Heat and Oxygen
D454-04	Standard Test Method for Rubber Deterioration by Heat and Air Pressure

Effect of Liquids

D3137-81 (2001)	Standard Test Method for Rubber Property—Hydrolytic Stability
D471-98	Standard Test Method for Rubber Property-Effect of Liquids
D1460-86 (2001)	Standard Test Method for Rubber Property—Change in Length During Liquid Immersion

Weathering

D518-99	Standard Test Method for Rubber Deterioration-Surface Cracking

Effect of Ozone

D1149-99	Standard Test Method for Rubber Deterioration-Surface Ozone Cracking in a Chamber
D1171-99	Standard Test Method for Rubber Deterioration-Surface Ozone Cracking Outdoors or Chamber (Triangular Specimens)

Mechanical (Stress relaxation in compression)

F38-00	Standard Test Methods for Creep Relaxation of a Gasket Material

A3.3 Composites

D5229/D5229M-92 (2004)	Standard Test Method for Moisture Absorption Properties and Equilibrium Conditioning of Polymer Matrix Composite Materials
C480-99 (2005)	Standard Test Method for Flexure Creep of Sandwich Constructions
C394-00	Standard Test Method for Shear Fatigue of Sandwich Core Materials
D6115-97 (2004)	Standard Test Method for Mode I Fatigue Delamination Growth Onset of Unidirectional Fiber-Reinforced Polymer Matrix Composites
D3479/D3479M-96 (2002)e1	Standard Test Method for Tension-Tension Fatigue of Polymer Matrix Composite Materials

A3.4 Adhesives

Thermal degradation

D1151-00	Standard Practice for Effect of Moisture and Temperature on Adhesive Bonds
D4502-92(2004)	Standard Test Method for Heat and Moisture Resistance of Wood-Adhesive Joints

Chemical resistance

D896-04	Standard Practice for Resistance of Adhesive Bonds to Chemical Reagents

Ageing

D1183-03	Standard Practices for Resistance of Adhesives to Cyclic Laboratory Aging Conditions

D3434-00	Standard Test Method for Multiple-Cycle Accelerated Aging Test (Automatic Boil Test) for Exterior Wet Use Wood Adhesives
D3632-98 (2004)	Standard Test Method for Accelerated Aging of Adhesive Joints by the Oxygen-Pressure Method
D2918-99	Standard Test Method for Durability Assessment of Adhesive Joints Stressed in Peel
D2919-01	Standard Test Method for Determining Durability of Adhesive Joints Stressed in Shear by Tension Loading
D3762-03	Standard Test Method for Adhesive-Bonded Surface Durability of Aluminum (Wedge Test)
D2295-96(2002)	Standard Test Method for Strength Properties of Adhesives in Shear by Tension Loading at Elevated Temperatures (Metal-to-Metal)
D4498-00	Standard Test Method for Heat-Fail Temperature in Shear of Hot Melt Adhesives

Fatigue

D3166-99	Standard Test Method for Fatigue Properties of Adhesives in Shear by Tension Loading (Metal/Metal)

Creep

D1780-99	Standard Practice for Conducting Creep Tests of Metal-to-Metal Adhesives
D2293-96 (2002)	Standard Test Method for Creep Properties of Adhesives in Shear by Compression Loading (Metal-to-Metal)
D2294-96 (2002)	Standard Test Method for Creep Properties of Adhesives in Shear by Tension Loading (Metal-to-Metal)
D4680-98 (2004)	Standard Test Method for Creep and Time to Failure of Adhesives in Static Shear by Compression Loading (Wood-to-Wood)

Appendix 4 Industrial Survey

A4.1 Industrial Sectors

Industrial sectors from which replies were received

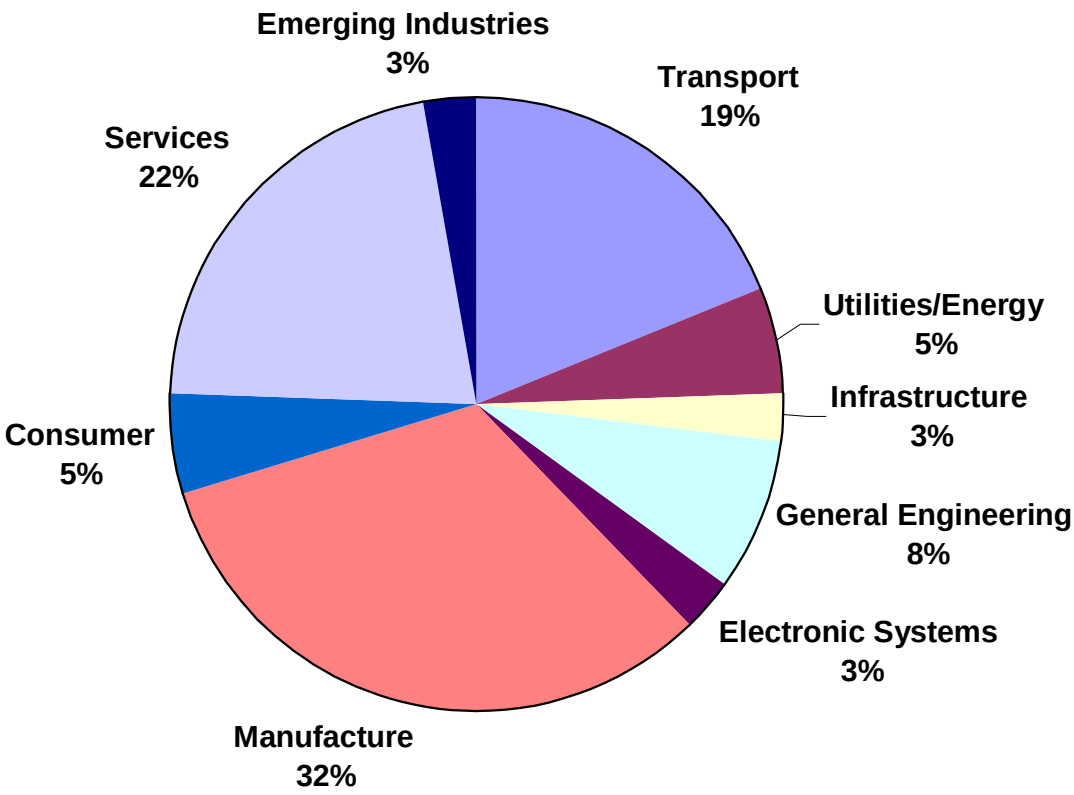

A4.2 Service Environment

What type of loads are the materials exposed to?

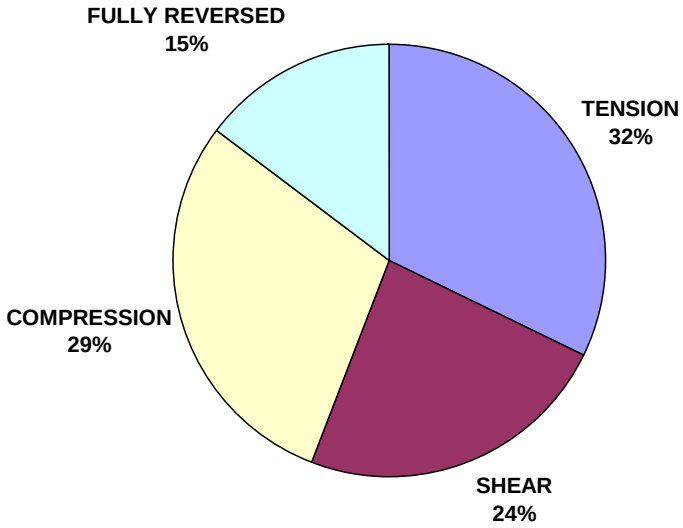

What periods of the exposure are experienced?

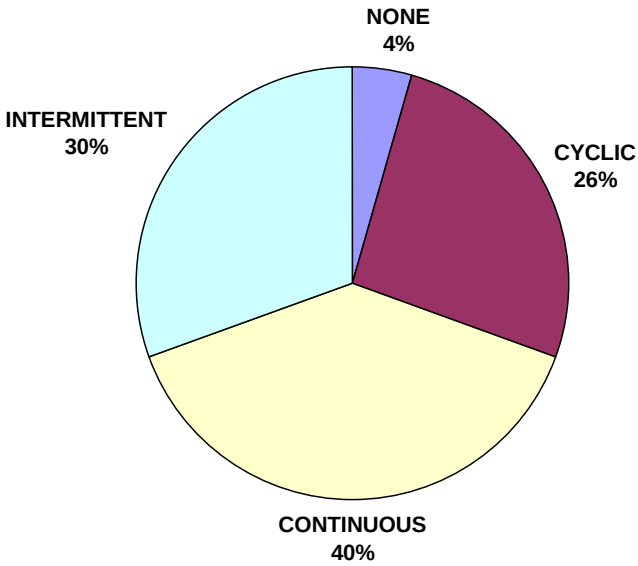

What chemical environments are the materials exposed to?

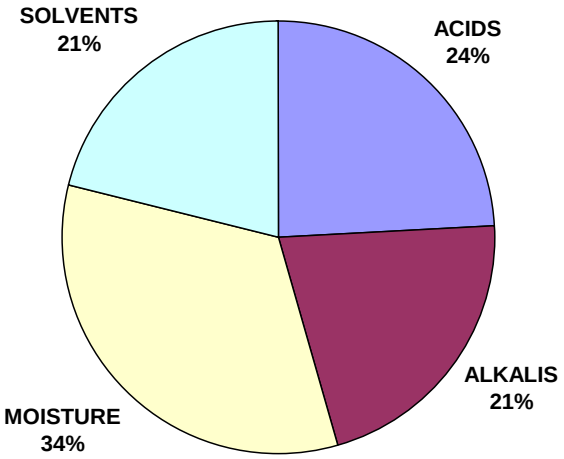

Alkali exposure

Chemical Environment	**Exposure**
Caustic soda	Splash
Medical drugs	Low concentrations
Calcium hydroxide	

Acid exposure

Chemical Environment	**Exposure**
Internal acids generated during heat degradation notably HCl from chloropolymers	Splash and vapour
Medical drugs	Low concentrations

Solvent exposure

Chemical Environment	**Exposure**
De-icing fluids: ethylene glycol, di-ethylene glycol, propylene glycol	Spray
Antifreeze solution	Vapour
Alcohols, aldehydes, ketones, ethers,	Exposure for 6 months or longer
Iso propyl alcohol	Long term, cyclic temperature exposure in the presence of solvents and ozone
Hydrocarbon fuels	
Aviation fuel, lubricating and hydraulic oils	
Water	
Commercial Solvents and Cleaning Products	
De-icing and cleaning fluids	

Are the loads applied at the same time (as the environment)?

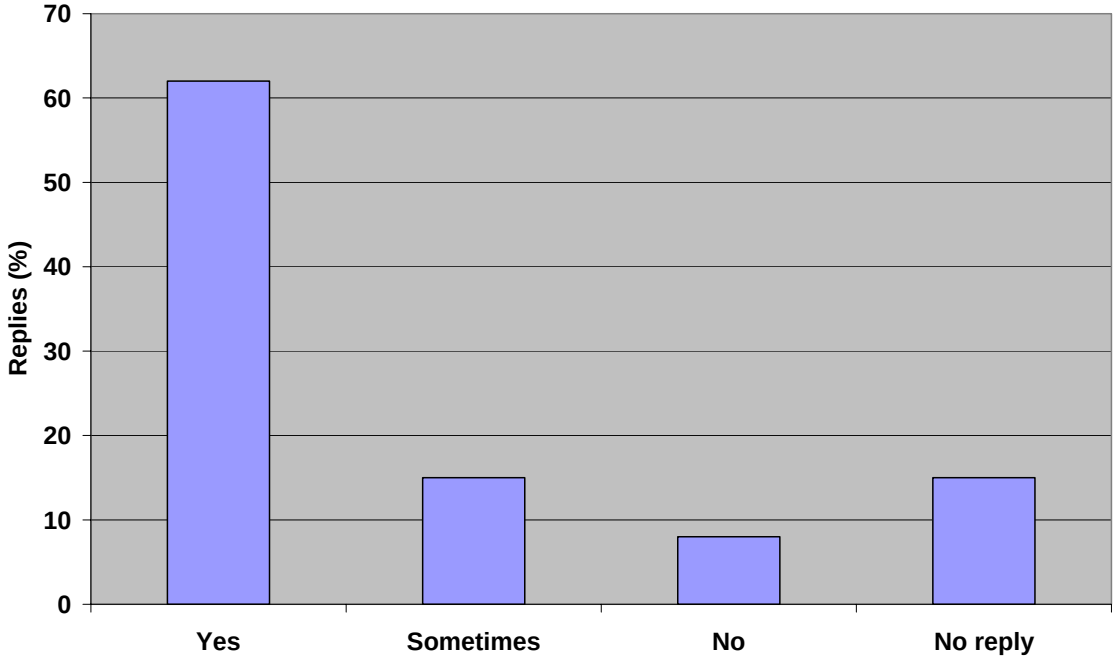

What materials are you interested in?

ABS
Acrylics
Polybutylene
Polycarbonate
Styrenics
Polyamides
Acrylics
Polystyrene
Polyurethanes
PVC plasticised and un-plasticised
Polyolefins: polypropylene, polyethylene
Polyesters: PET, PBT, PEN
Elastomers: synthetic latex, high performance rubber
Epoxy composites (CFRP, GFRP, Aramid)
Adhesives: thermoset, bismaelimide adhesives
EVA
Geosynthetics
High wear resistant fabrics
Thermoplastic pipes
Innovative materials

A4.3 Short-Term Testing

What short-term properties do you measure?
Tensile strength, UTS
Elongation
Modulus
Fracture energy
Impact
Hardness
Mass and dimensional changes
Visual appearance
Torsional strength
Resistance to climate cycling, heat, UV, chemical attack, wear
Environmental Stress Cracking tests
Immersion tests
Oven ageing tests
Retention of mechanical properties
Functional performance of the device
Burst pressure
Internal pressure tests in pipes with fluctuating fatigue loads in pressure cycles
Dynamic hot flex fatigue tests (100-150°C)

Do any of these relate to long-term performance?

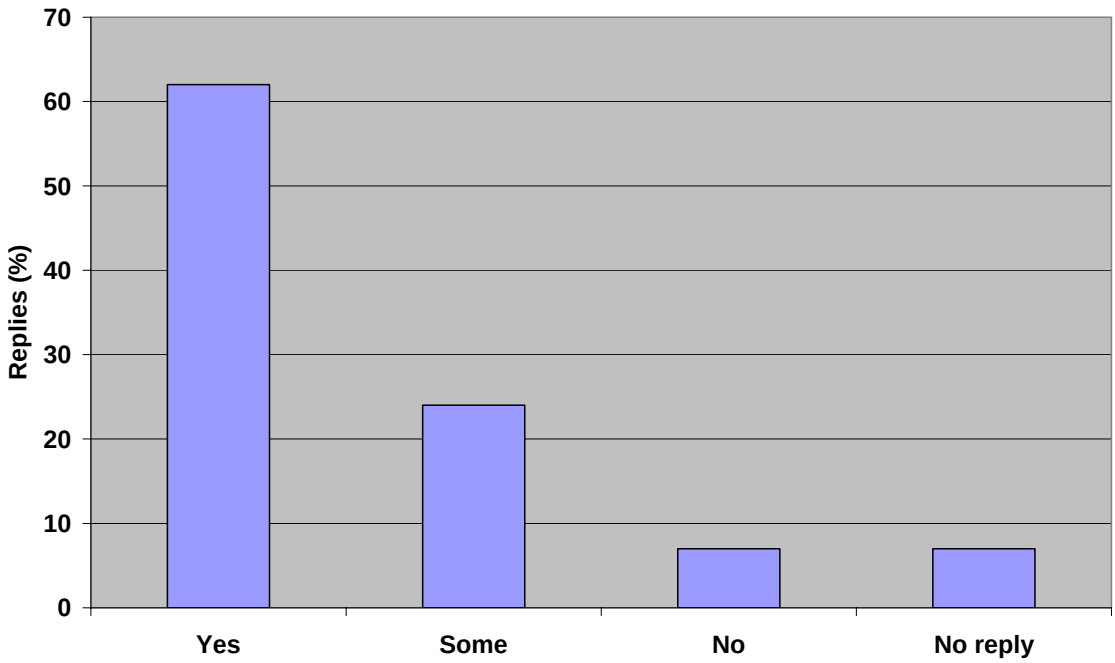

A4.4 Long-Term Testing

What long-term properties do you measure?

Lifetime in service until crazing becomes unacceptable
Long term burst hoop-stress
Fatigue strength (tensile and torsion of composites and bonded composite / metal joints). Compression fatigue of FW tubular suspension elements
Thermal stability
Resistance to climate cycling, heat, UV, chemical attack, wear.
Retention of mechanical properties
Functional performance of the device
Change in tensile, elongation, impact, appearance, hardness / modulus for 5000 hours.
Creep, creep-rupture, permeability, moisture diffusion
Colour fastness. Retention of physical properties
Long term shelf life tests - year at room temperature
Hardness, mass, dimensions, modulus, tensile strength

Are any of these covered by existing standards, reference methods etc?

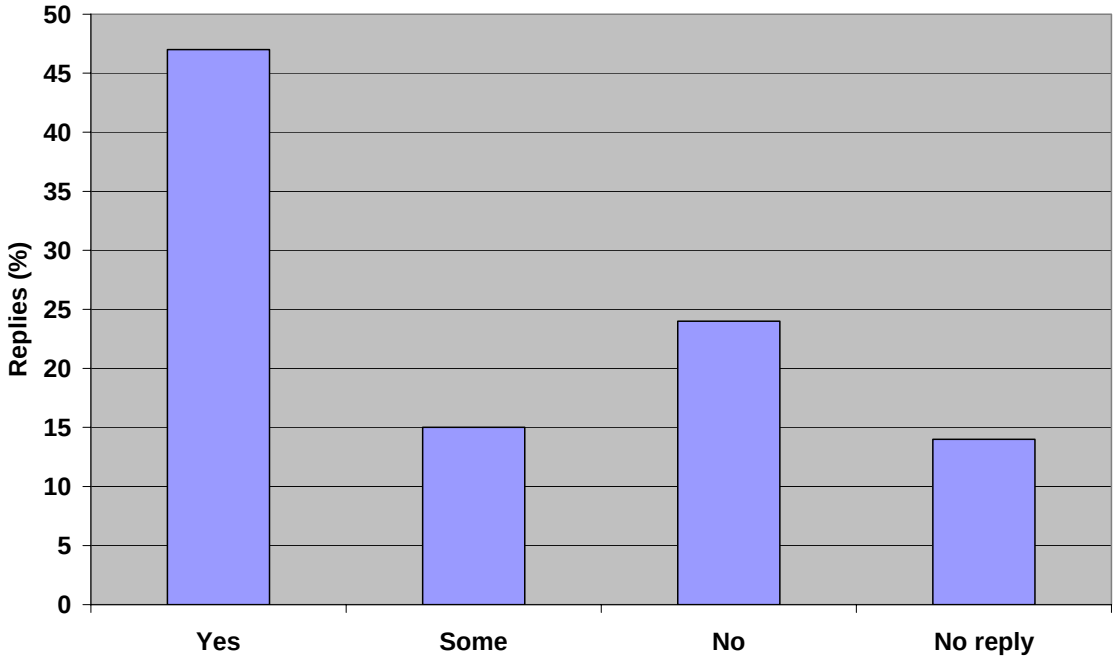

Standards used for testing include: BS, ISO, ASTM, SAE and internal standards.

A4.5 Accelerated Ageing

Do you use any accelerated ageing procedures?

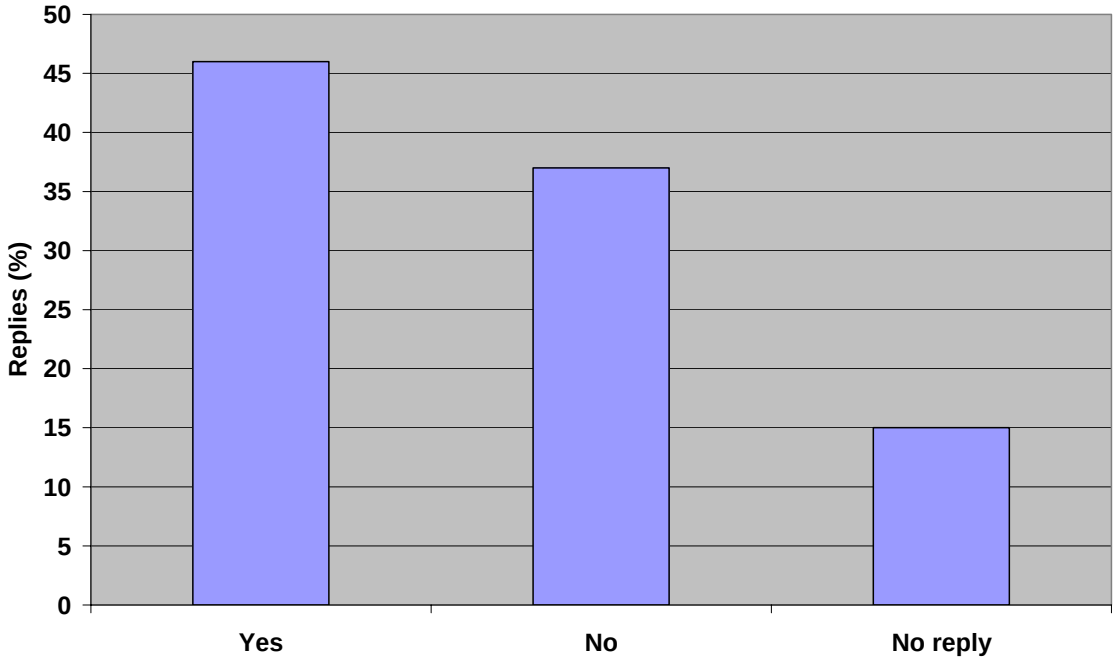

Are any of these covered by existing standards, reference methods etc?

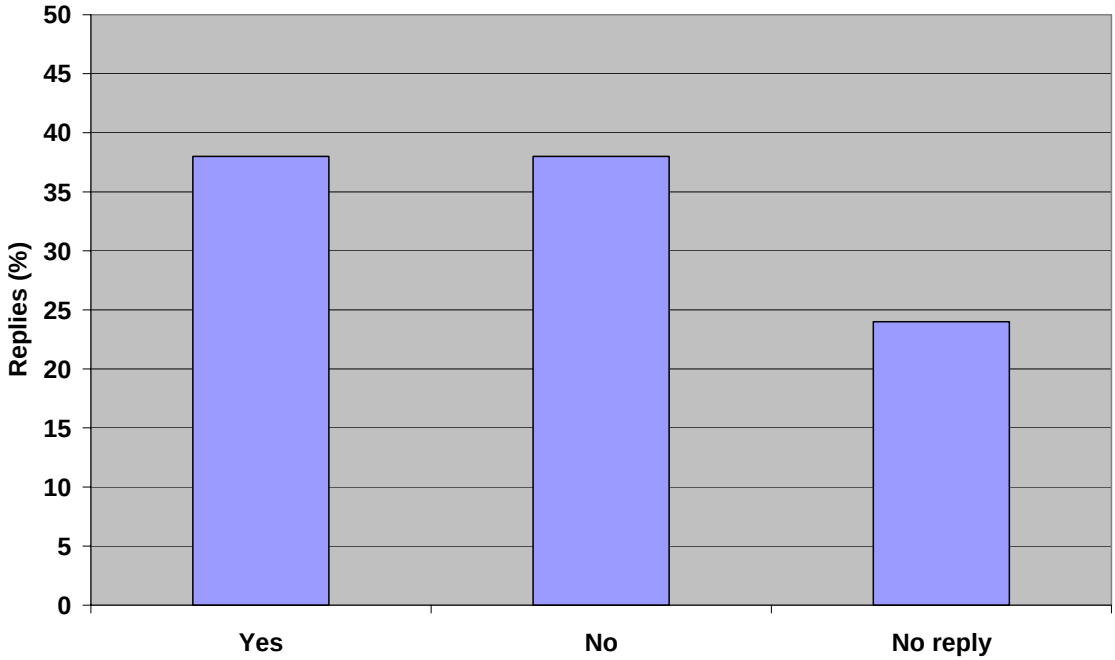

A4.6 Predictive Modelling

Do you use any predictive modelling to extrapolate the data and how far?

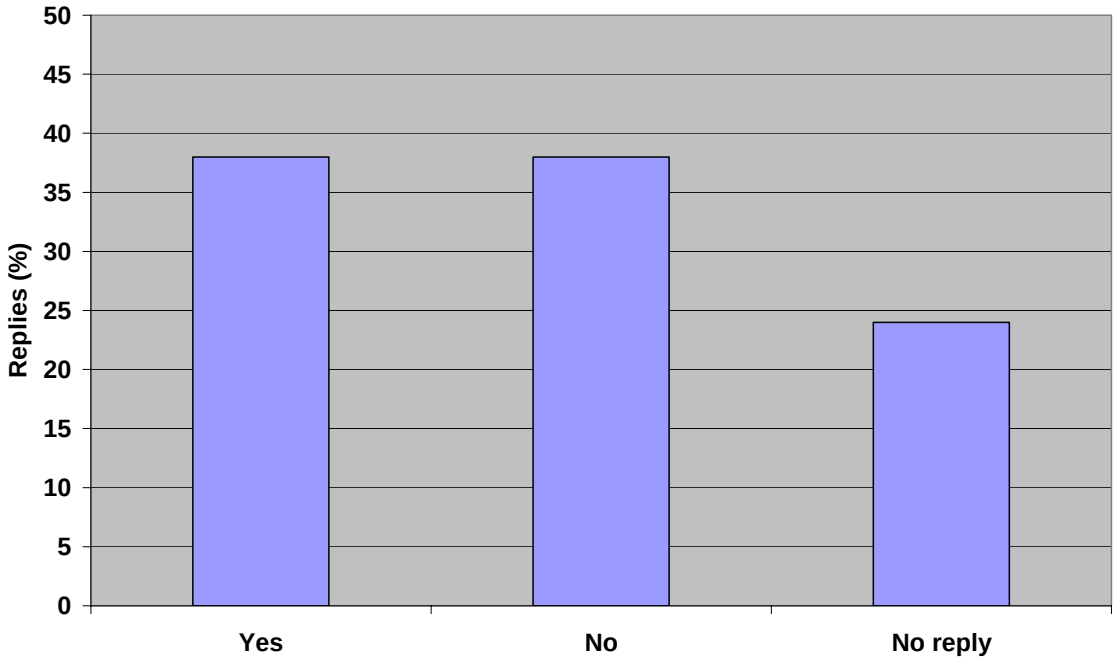

The lengths of time models are used to predict range between 5 and 100 years.
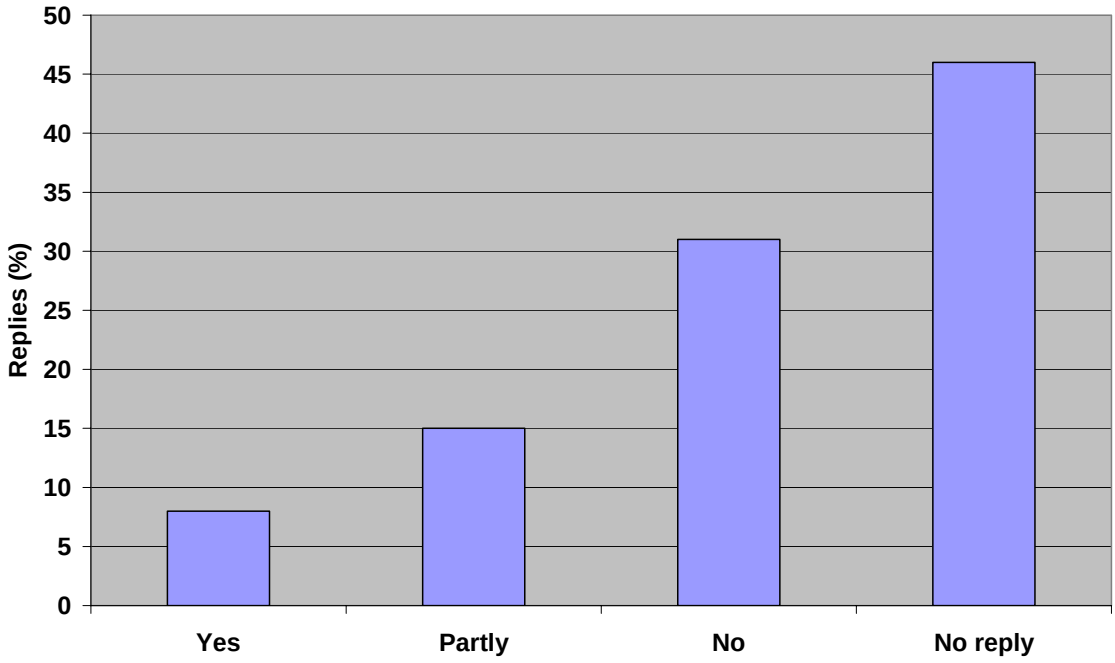
Have you validated the modelling procedure used?